JUNE 2017

M.Sc. in Civil Engineering

HAITHAM KHUDHUR ABBAS

GAZIANTEP UNIVERSITY

GRADUATE SCHOOL OF

NATURAL & APPLIED SCIENCES

IMPROVEMENT THE STRUCTURAL BEHAVIOR OF HOLLOW BEAM REINFORCED BY BOTH STEEL BARS AND FIBERS

M.Sc. THESIS
IN
CIVIL ENGINEERING

BY
HAITHAM KHUDHUR ABBAS BAJILAN

JUNE 2017

Improvement of The Structural Behavior of Hollow Beam Reinforced By Both Steel Bars And Fibers

M.Sc. Thesis

in

Civil Engineering

University of Gaziantep

Supervisor

Prof. Dr. Mustafa ÖZAKÇA

by

HAITHAM KHUDHUR ABBAS BAJILAN

June 2017

REPUBLIC OF TURKEY
UNIVERSITY OF GAZİANTEP
GRADUATE SCHOOL OF NATURAL & APPLIED SCIENCES
CIVIL ENGINEERING DEPARTMENT

Name of the thesis: Improvement of the Structural Behavior of Hollow Beam Reinforced by Both Steel Bars and Fibers.

Name of the student: Haitham Khudhur Abbas Bajilan

Exam date: 21/06/2017

Approval of the Graduate School of Natural and Applied Sciences

Prof. Dr. Ahmet Necmeddin YAZICI
Director

I certify that this thesis satisfies all the requirements as thesis for the degree of master of Science.

Prof. Dr. Abdulkadir ÇEVİK
Head of Department

This is to certify that we have read this thesis and that in our consensus opinion it is fully adequate, in scope and quality, as a thesis for the degree of master of science.

Prof. Dr. Mustafa ÖZAKÇA

Supervisor

Examining Committee Members:	Signature
Prof. Dr. Mustafa ÖZAKÇA	....
Assoc. Prof. Dr. Nildem TAYŞI	....
Assist. Prof. Dr. Derya BAKBAK	....

I hereby declare that all information in this document has been obtained and presented in accordance with academic rules and ethical conduct. I also declare that, as required by these rules and conduct, I have fully cited and referenced all material and results that are not original to this work.

Haitham Khudhur Abbas Bajilan

ABSTRACT

IMPROVEMENT OF THE STRUCTURAL BEHAVIOR OF HOLLOW BEAM REINFORCED BY BOTH STEEL BARS AND FIBER

BAJIlAN , HAITHAM KHUDHUR ABBAS
M.Sc. in Civil Engineering
Supervisor: Prof. Dr. Mustafa ÖZAKÇA
June 2017
102 Pages

The aim of the present experimental study is to examine the effect of steel fiber on the improvement of the structural behavior of hollow beams reinforced by both steel bars and fibers. This work is attempt to matching the both lightweight structural member with the structural ductility requirements. This is reached by combining the optimum beam's section topology with using steel fiber reinforcement. Therefore, different parameters are used to alter, named, shear span to depth ratio (a/d) and hollow shape. Three values for (a/d) used for investigating 8, 6, and 4. Two hollow type of circular and square shape are used. However, beam size, fiber type and longitudinal reinforcement ratio were left unchanged. All these parameters are compared with the control specimens of solid sections and hollow of normal concrete.

Keywords: Hollow beam; steel fiber; high strength concrete; lightweight structural member

ÖZET

DELİKLİ KİRİŞLERİN YAPISAL DAVRANIŞLARININ ÇELİK ÇUBUKLAR VE FİBERLER KULLANILARAK İYİLEŞTİRİLMESİ

BAJILAN , HAITHAM KHUDHUR
Yüksek LisansTezi, İnşaat Mühendisliğinde Bölümü
Tez Danışmanı: Prof. Dr. Mustafa ÖZAKÇA
Haziran 2017
102 Sayfa

Bu deneysel araştırmanın amacı, hem demir donatı hem de lifler ile takviye edilmiş içi boş kirişlerin yapısal davranışlarının geliştirilmesine çelik liflerin etkisini incelemektir. Bu çalışmada, hafif yapısal elemanlar elde ederken ihtiyaç duyulan yapısal sünekliğin sağlanması amaçlanmıştır. Buna, optimum kirişin kesit topolojisi ile çelik lif takviyesinin kullanılması ile ulaşılmıştır. Bu nedenle, kesme aralığının derinlik oranına (a/d) ve delik şekline göre farklı parametreler kullanılmıştır. (a/d) oranı olarak 8, 6 ve 4 olmak üzere üç değer araştırılmıştır. Ayrıca iki delik kesiti (dairesel ve kare) incelenmiştir. Bununla birlikte, kiriş boyutu, lif tipi ve uzunlamasına takviye oranı değişmeden bırakılmıştır. Bütün bu parametreler, normal betondan üretilmiş deliksiz ve delikli kontrol numunelerinin sonuçları ile karşılaştırılmıştır.

Anahtar Kelimeler: Delikli kiriş; çelik lif; yüksek mukavemetli beton; hafif yapısal eleman.

ACKNOWLEDGEMENTS

Praise and thanks a lot Allah Almighty, for giving me the health, knowledge and patience to complete this research. There were times that I had believed that this work would never end due to the ever increasing scope of work.

I would like to express my sincere thanks to my supervisor, Prof. Dr. Mustafa ÖZAKÇA for his invaluable guidance, advices, and supervision. I also appreciate the advice of the committee members.

My deep appreciation to my wife and my boys for their patience and patience throughout my studies and encourage me to continue my studies at the same time. I especially mention my wife and my great son Ammar for all his support. . Their love and support has encouraged me to complete my M.Sc. degree. I will always be grateful to my beloved family.

I am very grateful to my friend and brother Jumah Musdif Their for his continuous support and he is the one who encouraged me to work hard for finishing my M.Sc. degree.

I would like to thank Farid Hassun, Ahmed Abbas and Maan Abdel. And all brothers and friends. Due to their assistance with laboratory works. Finally, I wish you the best in everything that you do.

TABLE OF CONTENT

LIST OF TABLES

LIST OF FIGURES

Page

LIST OF SYMBOLS

ACI	American Concrete Institute
ASTM	American Society for Testing and Materials
SF	Steel Fiber
RC	Reinforced Concrete
FRC	Fiber Reinforced Concrete
SFHRC	Steel Fiber Hollow Reinforced Concrete
AR	Al kali Resistant
AR- GFRC	Al kali Resistant – Glass Fiber Reinforced Concrete
SNFRC	Synthetic Fiber Reinforced Concrete
SFRC	Steel Fiber Reinforced Concrete
HSC	High Strength Concrete
HPC	High- Performance Concrete
a /d	Shear Span to Depth Ratio
BC	British Columbia
U.S	United State
JSCE	Japanese Society of Civil Engineers
GFRC	Glass Fiber Reinforces Concrete
NFRC	Natural Fiber Reinforces Concrete
D	Dimensional
I_5,I_{10},I_{20}	Unity for Elastic

σ_f	First Crack Composite Flexural Strength
σ_{cu}	Ultimate Load Stage of Flexural Strength
V_f	Fiber Volume
v_u	ultimate shear strength
c	depth of compression zone above the tip of the diagonal crack
d	effective depth
F	fiber factor
L_f	fiber length
D_f	fiber diameter
ρ	amount of tensile reinforcement
COV	Coefficient of Variation
ν_f	Steel Fiber Ratio
LVDT	Linear Variable Displacement Transducer
N	Normal Concrete
S1	Steel Fiber Ratio (1 %)
80	Refer to square hollow size
C80	Refer to that circle radius equivalent to square
L	Beam Length
H	Beam Height
B	Beam Width
D	The effective depth of the beam
Fy	Yield Stress

Fu	Ultimate Stress
PC	Portland cement
W	Water
HRWRA	High Range Water Reducing Admixture
C	plain concrete
f_c'	compressive strength
f_t	tensile strength
P	applied load
D	diame length of cylindrical specimens
L	length of cylindrical specimens
HSFRC	high strength steel fiber reinforced concrete
CC	Conventional Concrete
SF	Silica Fume
NaPSS	Polystyrenesulfonate
w/c	Water per cement ratio
m	Mass
τ	Shear stress

CHAPTER 1

INTRODUCTION

1.1 Overview

The improvement in concrete technology and materials in the last 35 years has far exceeded that made through the last 150 years. Among much material used in concrete mix-up to enhance the concrete characteristics such as, supplementary cementing materials, super-plasticizing blend, and the new ingredient to concrete mixes is the fibers.

1.2 Background and Motivation

Concrete is a combination material consisting of cement, aggregate, and water which is formed by the chemical reaction of the cement and water output stone like structure. This material is a crisp once which is weak in tension but powerful in compression. The tensile ability of concrete is only a small portion about 10 percent of its compressive strength. Because of this, concrete will crack under small loads, at the tensile end region. Cracks initiated when the applied loads, temperature changes, or shrinkage concrete increase the tensile stresses in excess of the tensile capacity of the concrete. These cracks gradually increase in size and magnitude as the time elapses and finally makes concrete fail [1, 2].

The formation of cracks is the main reason for concrete failure. To increase the tensile strength of concrete many attempts have been made. One of the successful and most commonly used method is by providing steel reinforcement. These reinforcement must designed in such a manner to assure that the element will fail in a ductile manner and will provide warning before failure, and this what happened for flexural failure, but the issue with shear failure is different, that it is a brittle failure type and fails suddenly in nature because it does not give ample warning to inhabitants. This kind of failure happen generally, when a reinforced concrete beam is undergo to a combination of bending and shear force, with any little or no transverse shear reinforcement. Thus, to prevent such type of failure, beams are reinforced with adequate transverse reinforcement (stirrups). In public, the use of stirrups is costly because of the labor cost related with reinforcement installation. In addition, molding concrete in beams with closely-spaced stirrups could be troublesome and might lead to voids and linked poor bond between concrete and reinforcing bars. An alternative solution to stirrups is the use of randomly oriented fibers, the addition of Steel Fibers (SF) to concrete mix is known to increase its shear strength and, if adequate fibers are added, a crisp shear failure can be subdued in favor of ductile behavior [3, 4]. The use of deformed SF in place of minimum stirrup reinforcement is currently allowed in American Concrete Institute (ACI) Code Section 9.6.3, (ACI Committee 318, 2014) [5].

Fiber reinforcement act as crack arrestors and prevent the propagation of cracks, this concrete mix is named Fiber Reinforced Concrete (FRC). The main reason for adding fibers to concrete matrix is to improve to improve its energy absorption capacity and apparent ductility, and to provide crack resistance and crack control [6].

Motivation for the research: Many reports showed that, hollow and solid beams with same cross-section and same reinforcement fail almost at the same load when subjected to pure torsion with minimal effects of the internal concrete core. However, fewer works were found in the literature comparing the behavior of beams subjected to combined bending, torsion and shear.

Thus, the need for more experimental data for the behavior of Steel Fiber Reinforced Concrete (SFRC) hollow beam are the primarily motivations for this research. In particular, this research is aimed to match the both lightweight structural member with the structural ductility requirements and evaluate the structural behavior in SFRC hollow beams and the ability of SF to serve as replacement of minimum stirrup-type shear reinforcement.

1.3 Fiber Reinforced Concrete

FRC is concrete containing fibrous material which can increases its structural integrity. The basic fiber categories are glass, synthetics, steel and natural fiber materials as shown in Figure 1.1. These fibers have different geometrical characteristics (length, diameter, longitudinal shape, cross-sectional shape, and surface roughness).The selection of the type of fibers is dependent on the properties of the fibers such as Young's modulus, specific gravity, diameter, tensile strength etc. [3, 7- 9].

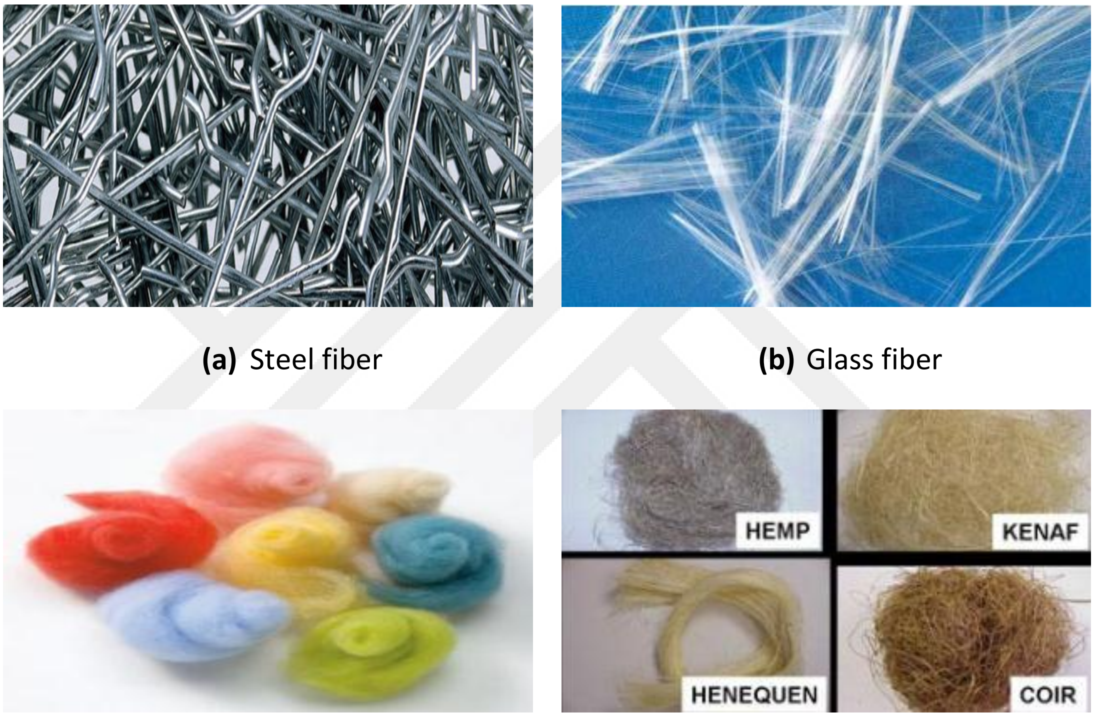

(a) Steel fiber

(b) Glass fiber

(c) Synthetic fiber

(d) Natural fiber

Figure 1.1 Basic fiber types.

Glass fiber is used in concrete mix for the first time in the USSR in the late of 1950s. The very high alkalinity (pH≥12.5) of the cement-based matrix make "E-glass and A-glass" composites types lose their strength rather quickly. Accordingly, these composites were unsuitable for long-term use. Continued research, however, resulted in the development of a new alkali resistant fiber that provided improved long-term durability. The new system was named alkali resistant-glass FRC.

The major uses of glass FRC are in architectural precast concrete and exterior building facade panels. This material is very good in making shapes on the front of any building and it is less dense than steel.

Natural fibers are one of the oldest forms of fiber-reinforced composites, which can be obtained at low levels of cost and energy using locally available workers and technical knowhow. However, one of the main disadvantages of using these forms of fibers is their proneness to disintegrate in an alkaline environment. To overcome these disadvantages and to improve their durability they used admixtures and applying special treatment to the fibers.

Example of the natural fibers are coconut fiber, sisal fiber, sugar cane, bagasse fiber, bamboo fiber, jute fiber, flax, elephant grass. Such fibers are increase toughness and flexural strength. It also induces good durability in concrete. Natural FRC is suitable for low-cost construction, which is very desirable for developing countries such as low-cost house construction, non-pressure pipes, roof tiles, and flat and corrugated panels.

Synthetic fibers specifically engineered for concrete and are man-made textile fibers including usually those made from natural materials and resulting from research and development in the petrochemical and textile industries. Synthetic fibers are added to concrete mix before or during the mixing operation, and the use of synthetic fibers at typical rates does not require mix design changes. Synthetic fibers types are nylon, acrylic, carbon, polyester, aramid, polypropylene and polyethylene.

Among the various types of fibers, SF, are most widely used in the concrete industry. Steel fiber is rounded fibers (typically diameter may vary from 0.20 to 0.75mm), also it is short fiber (typically from 12.7 to 63.5 mm), generally deformed to improve bond with concrete. The use of SF in the concrete mixes has gained popularity in the construction industry in the last two decade due to the improvement in the mechanical concrete properties after its addition to the mix. Studies have demonstrated that the addition of SF can improve many of the concrete properties such as, tensile resistance, ductility, crack control, and fracture toughness.

SFRC has been used in various types of structures; for example in construction of bridge deck overlays, industrial floors, airport runways, highway pavements, tunnel linings, spillways, dams, etc. However, the use of SFRC in buildings has been very limited, even though SF have been shown to enhance the flexural and shear behavior of concrete members. The limited use of SFRC in building structures is primarily due to the lack of design provisions in building codes.

1.4 High Strength Concrete

ACI defines a high-strength concrete as concrete having a specified compressive strength for design of (41 MPa) or higher. ACI defines high-performance concrete as "concrete meeting special combinations of performance and uniformity requirements that cannot always be achieved routinely when using conventional constituents and normal mixing, placing and curing practices" [10].

Thus, the need for more experimental data for the behavior of large high strength SFRC beams the little knowledge on the behavior of SFRC hollow beams are the primarily inspirations for this research. Very few attempts have been made to study the effect of using SF in the behavior of SFRC hollow beams. The interaction between the beam capacity, steel fiber, shear span to depth ratio (a/d), the transverse shear reinforcement, and the lightweight member needs more investigation in order to establish comprehensive understanding, and to be able to design hollow reinforced concrete beams with SF.

1.5 Purpose of the Study

Prior to listing the objectives of this research, the statement of the problem is presented. In spite of good results obtained from improving the behavior of structural members using different materials, but there are wide area of investigation remain with uncertainty.

Such as, investigation of the effect of applied load's location and shape of hollow, Therefore, the ***problem statement*** can be summarized as follows;

1. From structural angle of view, concrete has heavy self-weighted, which is undesired in high-rise building. Moreover, concrete shows high brittleness behavior, that is required another materials to improve its ductility.

2. From economy angle of view, there are significant area with zero and low stress, this area can be eliminated using optimum section.

This proposed work is attempt to matching the both lightweight structural member with the structural ductility requirements. This can reach by combining the optimum beam's section topology with using steel fiber reinforcement. Therefore, different parameters are used to alter, named, shear span to depth ratio (a/d) and hollow shape. Three values for (a/d) used for investigating 8, 6, and 4. Two hollow type of circular and square shape are used. All these parameters are compared with the control specimens of solid sections and hollow of normal concrete.

The experimental data presented in this thesis is a part of the experimental work of the Ph.D. thesis of "Ahmmad A. Abbass" with title "Mechanical and structural behavior for fiber and engineered cementitious composites hollow sections for structural members" which was carried out in the laboratories of the Civil Engineering Department/Gaziantep University.

1.6 Thesis Layout

The present research work investigate, experimentally, the effect of adding steel fiber on the behavior of hollow high strength reinforced concrete beams, the introduction for this work is presented in Chapter 1.

Chapter 2 represent a literature review on behavior of SFRC beams, the historical development of fiber and general definition of the steel fiber.

Chapter 3 deals with the experimental program. Test specimens description, detail of reinforcement, specimen construction, and material properties are presented

Chapter 4 presents results of the experimental testing and observations. Discussions and comments relevant to the results are included also in this chapter.

Chapter 5 summarizes the general conclusions of the present work along with recommendations for future studies and developments on performance of SFRC elements.

CHAPTER 2

LITERATURE REVIEW

2.1 Introduction

This chapter illustrates an understanding of the developments in the study of FRC. At first, the historical development of fiber and general definition of the SF will be presented, as a lead-in to the discussion about how the SF effect on concrete mechanical properties. Next, the compression, tension, flexural, and shear behavior of SFRC based on previous analytical and experimental investigations will be discussed in brief.

2.2 History and Features of Fiber Reinforced Concrete

The idea of making the behavior of concrete better in tension by controlling the propagation and opening of cracks with discrete fibers distributed randomly throughout the matrix is not new. In the past, fibers have been used to reinforce brittle materials. In BC, horsehair was used to reinforce mortar and plaster. Iraqis used reed mats within the clay bricks layers to build the ziggurat at Aqar Quf. Egyptians used straw in mud masonry to strengthen the construction materials, also, the oldest house in the U.S. was built with sunbaked adobe reinforced with straw. [3, 11, 12]

In the early 19th century, asbestos was used in the concrete to prevent it from formation of cracks. However, in the late 19th century, primarily due to health hazards accompanied with asbestos fibers and because of the arising concern in the importance of structural behavior, a great attention was paid to more understanding the behavior of the FRC and alternative fiber types were introduced throughout the 1960s and 1970s to enhance the concrete's most significant properties [13-15]. The improved properties of concrete mix due to using the fibers included as listed by the report of ACI committee 544 [3]. The importance of adding fiber was proven by a large number of research results showing the improvement of these properties and durability of concrete by adding fibers [3, 16-19].

As mentioned in Chapter 1 Section 1.3, there are different fiber types in the market proposed to address various design requirements and constraints. The mechanical properties of commonly used fibers in concrete mix is presented in details at reference [23].

Among the various types of fibers, SF are most widely used in the concrete industry, and the first commercial SFRC pavement in the United States was placed 1971 at a truck weighing station [23]. The usefulness of SFRC has been aided due to developments in the SF filed which led to many new SF types have been produced, and the developments in the concrete field which led to high-range water-reducing admixtures “super plasticizer” increase the workability of SFRC.

Modern studies and worldwide interest in the subject began during the early 1960’s, in which the first major attempt was made to investigate the potential of SF as a reinforcement for concrete [20]. Following that initial work, a lot of researches, experimental works, and industrial applications of SFRC have been done. These interests and continuous researches led to standardization for measuring of properties, testing, specifying, proportioning, mixing, placing, and design methodologies for FRC presented in three reports by ACI Committee 544 [10, 21, 22]

In the present work SF has been used to improve the behavior of concrete mix, the definition of the SF and the properties of SFRC is presented in the next section.

2.3 Steel Fiber Reinforced Concrete

2.3.1 General Definition

SFRC is largely used in many of civil engineering applications. It is a composition of cements, aggregate, and a dispersion of discontinuous, small SF. It may also contain admixtures “super plasticizer” commonly used with conventional concrete. The wide range uses of SFRC are due to economic decisions and experience with conventional steel reinforcement [24, 25].

The addition of SF to concrete mix improves the post-cracking behavior of SFRC significantly compared to plain concrete. This happens by the “bridging action”. Figure 2.1 illustrates the primary role of SF in which it acts to bridge cracks due to tension in the concrete [26]. Depending on bond strength, the fibers fail in two manners, either by fracture of SF or pull out of the concrete as cracks open or by pulling out resistance of fibers, which is more favorable because SFRC will be more ductile and absorb a greater amount of energy prior to a complete failure. Figure 2.2 present the fracture surface for SFRC.

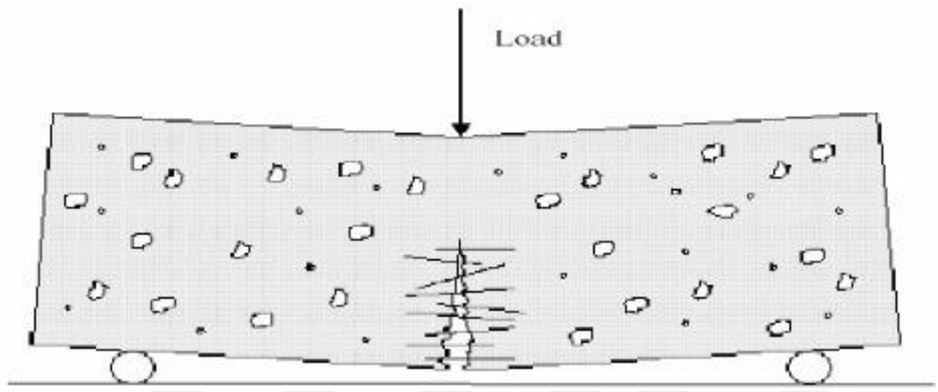

Figure 2.1 Pullout mechanism for SFRC [26]

Figure 2.2 Fracture Surface of SFRC[26]

Thus, the addition of SF improves the ductility of the concrete mix, as shown in Figure 2.3. Flexural strength, fatigue strength, and also resistance to cracking and spelling are improved.

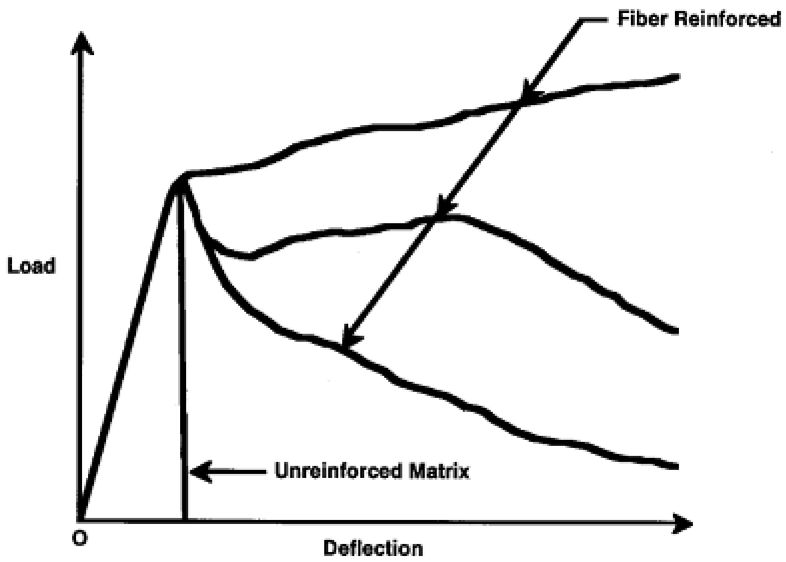

Figure 2.3 Load - deflection curves for FRC and unreinforced [3]

The extent of improvement in the concrete mix properties and the performance of SFRC are greatly dependent and vary based on the quantity (SF content) and type of fibers (fiber geometry, aspect ratio, and bond characteristics) used and the quality of the concrete mix [27-29].

The defect of using SF in concrete mix is the reduction in workability. Workability is defined as "that property of freshly mixed concrete which determines the ease and homogeneity with which it can be mixed, placed, consolidated, and finished to a homogenous condition." [30-32].

SF are defined as short fiber with the length varies from 0.25 in. (6.4 mm) to 3 in. (76 mm), having an aspect ratio (ratio of length to diameter) from about 20 to 100, The most common fiber diameters are in the range of 0.017 in. (0.45 mm) to 0.04 in. (1.0 mm). [3, 21, 32], as shown in Figure 2.4, SF are sufficiently small to be randomly distributed in an unhardened concrete mixture using usual mixing procedures.

The important properties of SF are strength, stiffness, and the ability of the fibers to bond with the concrete. SF have high tensile strength about (345-3000 MPa) and high modules of elasticity (200MPa), these fibers are protected from corrosion by the alkaline environment of the cementations matrix. The primary source of bond for these fibers comes from the friction between the fibers and concrete. Therefore, to enhance bond, one can choose fibers with a higher surface area to volume ratio. Thus, fibers with rectangular sections are more efficient than fibers with circular sections and for the same fiber length, fibers with smaller diameters (higher aspect ratio) are more efficient.

Figure 2.4 Different types of SF

The SF are classified either, based upon the product used in their manufacture, 'this classification based on ASTM A 820 [33]" for four general types: cold-drawn wire, cut sheet, melt-extracted and other fibers.

Alternatively, The Japanese Society of Civil Engineers (JSCE) classified SF based on the shape of their cross-section, for three types [3]:

- Square section.
- Circular section.

- Crescent section.

Various steel fiber geometries are shown in Figure 2.5. Usually, the quantity of SF ratio ranges from (0.25- 2%) by volume [21, 32]. The low ratio of the range used for some precast applications, and composite steel deck toppings. The upper ratio is common for safety applications (safes, domes, etc.).

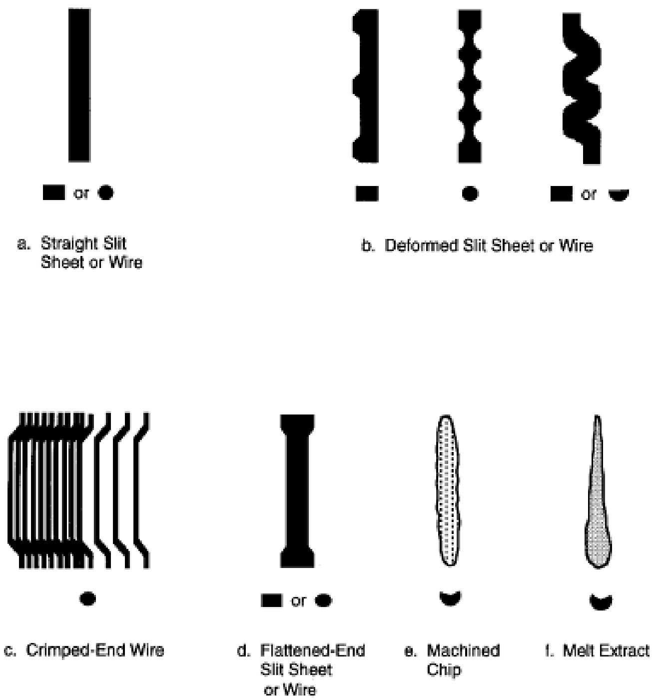

Figure 2.5 Various SF Geometries [3]

Understanding the mechanical properties of SFRC is very important feature for a successful design and their variation with fiber amount and type. These properties are presented in the proceeding sub sections of this chapter.

2.3.2 Properties of steel fiber reinforced concrete

The quality of concrete is affected by many factors like properties of cement, fine aggregate, coarse aggregate. Addition to that, the FRC depends on type of fiber, aspect ratio, quantity and orientation of fiber.

2.3.2.1 Type of fiber

A better fiber to use is the one that possess the following qualities: good adhesion within the matrix, adaptable elasticity modulus (sometimes higher than that of the matrix), compatibility with the binder (which should not be attacked or destroyed in the long term) and an accessible price, taking into account the proportion within the mix. In the early days of SF reinforcement, most of the fibers used were straight and smooth; but now there are different types of SF straight, crimped, end-hook, end paddles, etc.

Naaman and Najm [34] and Trottier and Banthia [35] from their experimental results with study of the effect of fiber types concluded that, fibers with end deformed shape provide significant improvements in the toughness and energy absorption capabilities with higher resistance to pullout than smooth fibers. Moreover, they also indicated that fibers with end deformations are more effectual compared to fibers with deformations along the whole length

Soroushian and Bayasi [36] found that hooked fibers improved some mechanical anchorage and are more effective than straight fibers, also hooked fiber generate energy absorption capacities and flexural strengths which are higher than those of crimped and straight fibers

Wu, et al. [37] investigated the effects of fiber type using three shaped steel fibers (straight, corrugated, and hooked-end) on the workability, compressive strength, and flexural behavior of SFRC. They concluded that the workability decreased by 45.1% and 51.2% for hooked-end and corrugated fibers respectively in comparison with the use of straight fibers. They concluded that, the use of hooked end SF has superior improvement to the mechanical properties in comparison of the other SF shapes used in their work.

2.3.2.2 Aspect ratio

Aspect ratio is defined as the ratio of the fiber length to width or diameter of the fiber. According to the Building Code Requirements for Structural Concrete ACI-318M [5] limits the aspect ratio of SF to not smaller than 50 and not greater than

100. Generally, the raise in aspect ratio increases the strength and toughness until the aspect ratio of 100. Short SF with an aspect ratio less than 50 are not able to interlock and can easily be spread by vibration. On the other hand, above the ratio of 100 the strength of concrete decreases, in view of reduced workability and compaction. Due to the fact that, SF with an aspect ratio greater than 100 will tend to interlock to form a ball, which is very difficult to separate by vibration alone.

From investigations [6, 14, 25, 29, 38, 39], it can be determined that the higher the aspect ratio, the greater the ability of SF to transmit tensile stresses across a crack. The fiber with higher aspect ratio means the fiber has a large surface area to engage a small volume of steel through bond action with the concrete. This leads to a stiffer fiber with improved composite action, because the increase in the length of SF leads to a stronger bond between SF and concrete, which increases the ability of SF to transmit tensile stresses across a crack.

2.3.2.3 Fiber quantity

Generally, fiber content in concrete is measured as a percentage of total volume. When the percentage of fiber is higher, this leads to improve the strength and toughness of concrete.

ACI committee 544 [3] provides trial mixes and the maximum fiber content. The report also mentioned that for good workability the SF content are available from the SF manufacturers. The report stated that, the typical SF content is from 0.5 to 1.5 volume percent for SFRC mixture with normal mixing and placement procedure. However, higher percentages of fibers (from 2 to 10 volume percent) are used with special fiber addition techniques and placement procedures

Rossi et al. [40] reported that the addition of SF increases the critical load required to reach the outset of macro crack significantly. They mentioned that to avoid difficulties during placement, a 1% content of these long fibers would be an upper bound.

Zollo, [41] showed that when a high percentage of fiber is added to concrete, it requires special mixing and placing to ensure regular distribution of fiber and coarse aggregate in casting. In his article he provides Figure 2.6 which present a summary of the basic fiber types, their ranges of commercial application, including the high, moderate, and low regimes, and the associated production methods.

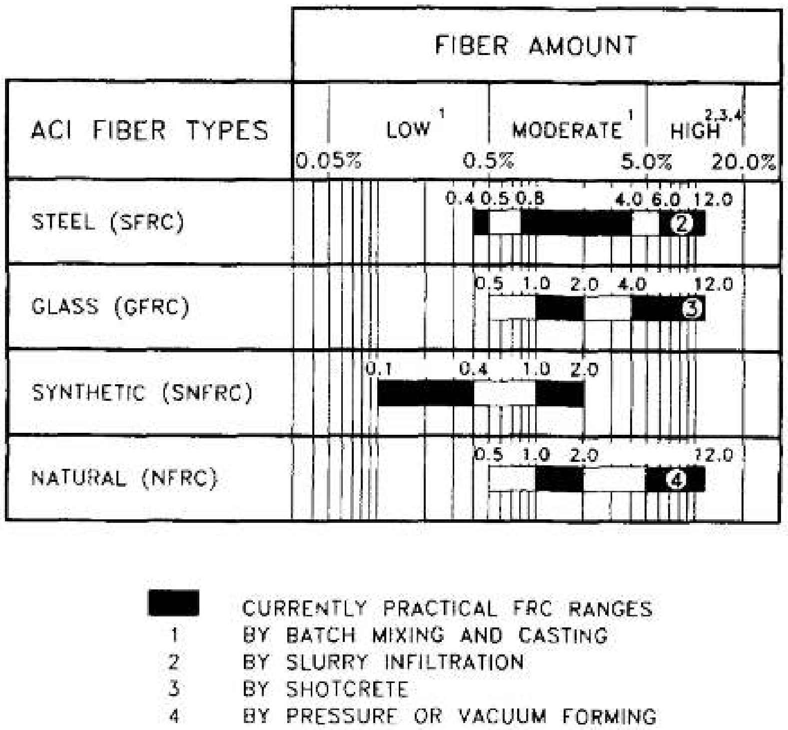

Figure 2.6 Fiber types and amount used by volume per cent of concrete mix [41].

Jain and Singh [42] showed that concretes containing low fiber volume contents greater than or equal to 0.5% led to multiple cracking while using SF volume content from 0.75 to 1.0% observed satisfactory shear performance.

Wu, et al. [37] investigated the effects of fiber contents by volume using three ratios 1%, 2%, and 3% on mechanical properties of SFRC. Their results indicated that the increase in fiber content could gradually decrease the workability of the mixture. With 1%, 2%, and 3% straight fibers, the workability decreased by 14.9%, 25.6%, and 38.1% respectively. The decreasing of the workability with the SF content are shown in Figure 2.7.

Wu, et al. [37] concluded that the increase of fiber content increase both the compressive and ultimate flexural strengths (see Figure 2.8).

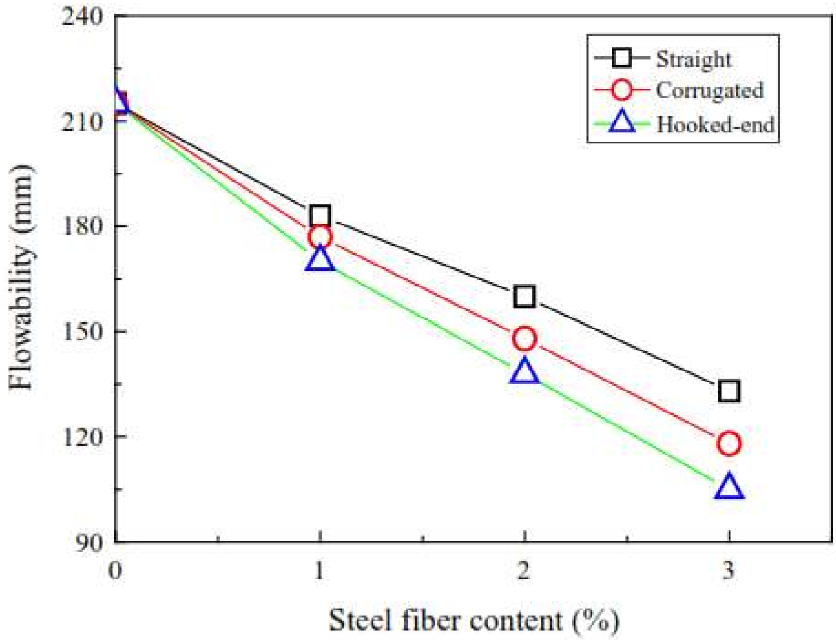

Figure 2.7 Effects of SF content and shape on workability of concrete mix [37]

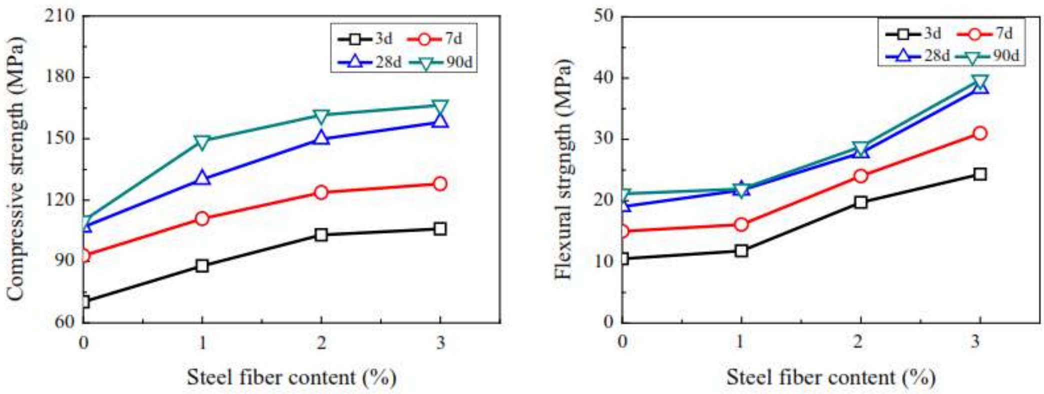

Figure 2.8 Effects of SF content on strengths of concrete mix [37].

2.3.2.4 Orientation of fiber

The orientations of fibers play an important role in determining the capacity of concrete. In reinforced concrete, the reinforcements are placed in desired direction. The FRC will have maximum resistance when all fibers are oriented parallel to the tensile stress developed.

Johnston [14] stated that, the short fibers tend to assume a more random orientation which lead to more uniform distribution of fibers in the mix. However, even with using these type of short fibers, the distribution is rarely completely uniform, and their orientation is not preferably random. The mixing and placement process are largely effected the uniformity of volume distribution of the fibers, and in practice a uniform distribution is rarely achieved. Figure 2.9 shows the distribution of steel fibers in concrete as observed by X-ray, showing non-uniform distribution.

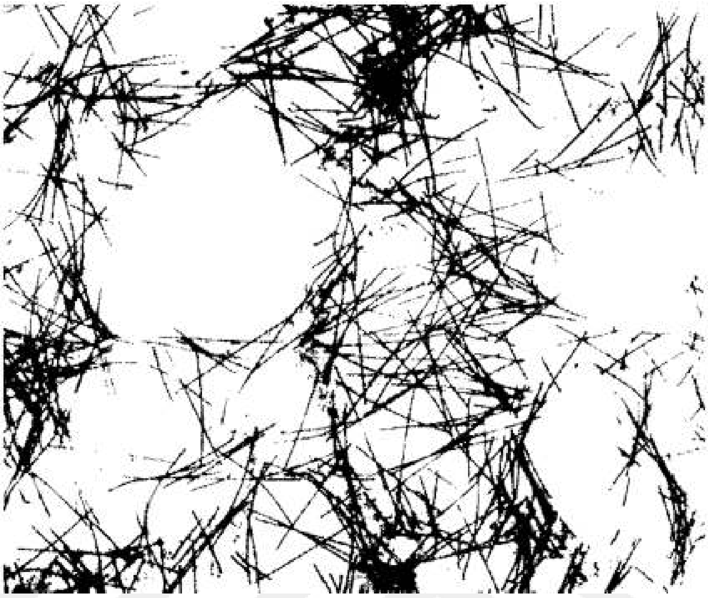

Figure 2.9 Non-uniform distribution of SF in concrete as observed by X-ray [14].

The large ratio of the fiber length to the thickness will lead to a 2D distribution of the composite, which is usually the case in thin cast overlays. A preferred 2D distribution can also be promoted in thick cast due to vibration. This will give rise to anisotropic behavior.

Bentur and Mindess [43] dealt with the orientation of fiber, which will follow on one of the following three cases: 1D, 2D, or 3D. Most models assume a 1D-fiber orientation, where the fibers are loaded in direct tension. In design of conventional reinforced concrete which uses continuous reinforcement, engineers typical design is for 1D (tension steel in beams and one-way slabs) or 2D (tension steel in two-way slabs) orientations. However, in the case of discrete fibers it is more common to assume 2D or 3D orientations, because the short discontinuous fibers tend to rotate during pouring and/or curing processes. This often leads to reduced fiber efficiency in un-cracked and cracked situations. However, in a cracked section, orientation leads to local bending in the fiber, which can lead to improved efficiency.

Torrents [44] presented a practical method to measure, non-destructively, the amount and orientation of fibers for SFRC, from their experimental test observation they mentioned that, the SF do not distribute uniformly in the three direction for SFRC result in anisotropic material. The fiber orientations in the concrete matrix occur as a result of several aspects, they conclude that the two most significant aspects affect fiber orientation are the wall-effects introduced by the formwork “fibers tend to orientate parallel to the boundaries (see Figure 2.10)” and the fresh state properties of SFRC,

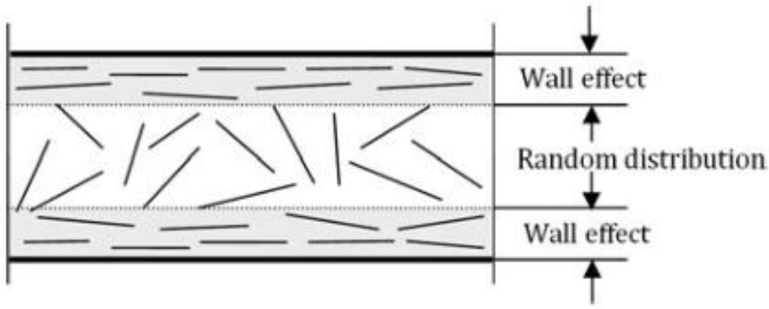

Figure 2.10 Favored orientation (wall-effect) in a thin element [44].

Their conclusions confirm that fibers align with the flow of fresh concrete and the alignment has a direct influence on the bending strength (better fiber-alignment leads to a higher bending strength). While, large scatter in the results of bending strength resulted in conventional SFRC (non-self-compacting concrete), decreasing the characteristic values of strength

2.4 Compressive Strength of Steel Fiber Reinforced Concrete

The survey study indicate that, the presence of the SF has slightly affect the compressive strength of concrete, but overall effect is negligible in many cases. Many researchers [45-47] have observed increases in the compressive strength of concrete ranging from 0 to 15% for up to 1.5 percent by volume of fibers. while other researchers observed that, the increase in the compressive strength range from negligible in most cases to 23% for SFRC for up to 2.0 percent by volume of fiber [10, 48]

The key role of SF is to reduce the rate of strength loss after the peak stress. Several researchers [49-52] studied experimentally the compressive stress-strain behavior of

SFRC mixture. Typical stress-strain curves for SFRC in compression are shown in Figure 2.12. One can observe from these compressive stress-strain relationships for SFRC that, a substantial increase in the strain at the peak stress and the modified unloading branch (i.e., less steep descending branch than that of normal concrete without SF).

That means the addition of SF improves the toughness of SFRC in compression, where toughness is energy absorption ability during deformation and it can be obtained from and this incensement in toughness is useful in preventing sudden failure under static loading.

In addition, it can be seen from these curves that as the volume fraction and the aspect ratio of SF increase, the area under the compressive stress-strain increased (i.e., led to a less steep descending branch for the curves), this is indicative of substantially higher toughness in compression.

Hughes and Fattuhi [53] examined experimentally effects of the addition of SF on the compressive stress-strain properties. They concluded that the addition of 0.25 x 25 mm SF leads to the maximum increase in the compressive strength of the concrete of nearly 7%.

Fanella and Naaman [54] studied stress-strain properties of SF reinforced mortar in compression. The test results showed that the stress-strain curves presented in Figure 2.14 for the FRC diverge slightly on the ascending portion of the curve and considerable divergence was observed on the descending portion.

Otter and Naaman [55] showed that, using the SF in low strength concrete increase their compressive strength significantly compared to plain concrete, additionally, they mentioned that, the strength is directly related to volume fraction of SF used. The addition of SF to concrete affects the compressive stress-strain curve, these fibers make the slope of the descending branch less steep. The slope of the descending part as shown in Figure 2.13 is decreased as the amount of SF increased.

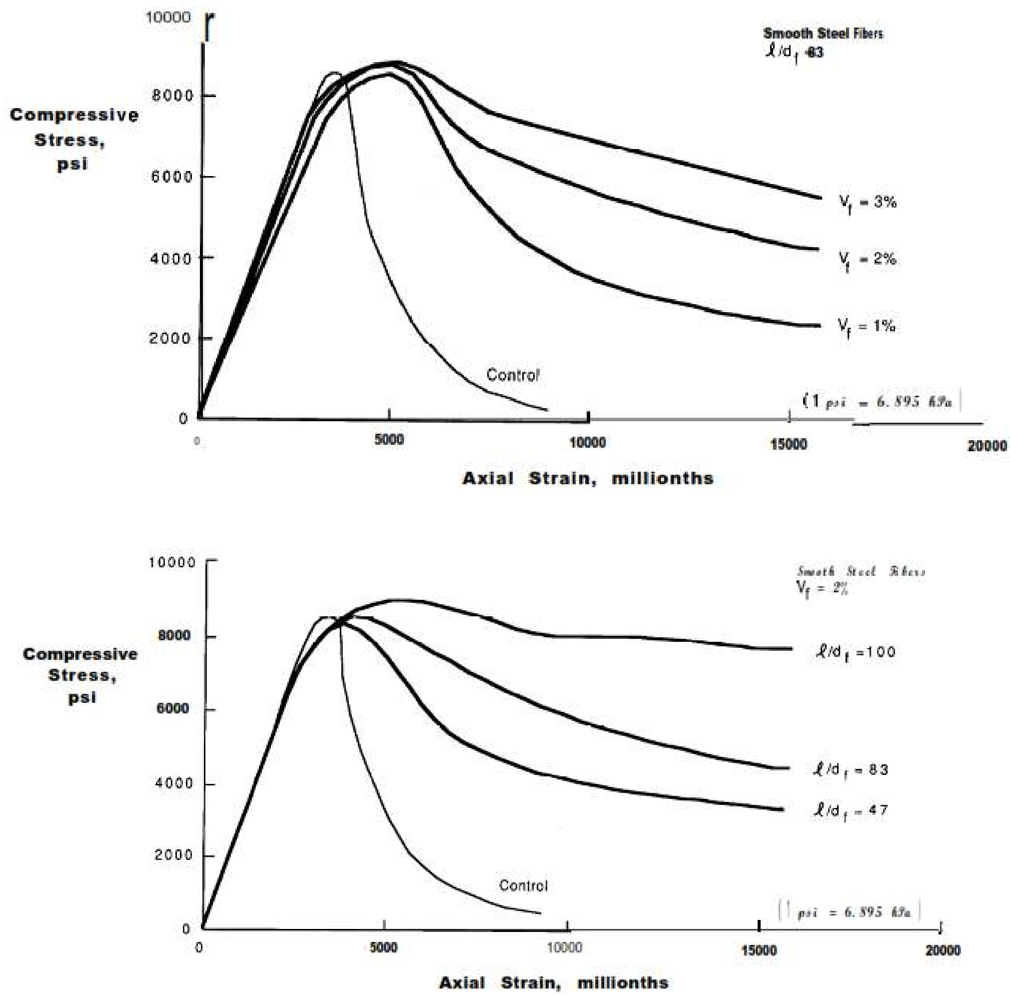

Figure 2.11 Typical stress-strain curves for SFRC in compression [10].

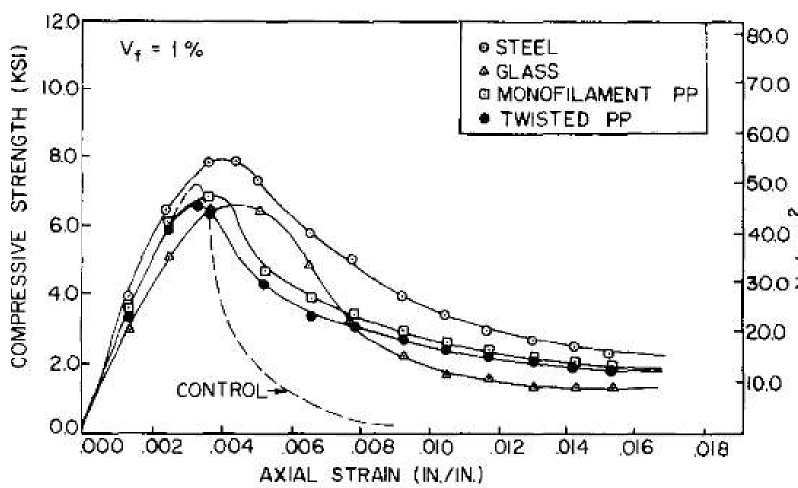

Figure 2.12 Typical compression stress-strain curves of FRC [53]

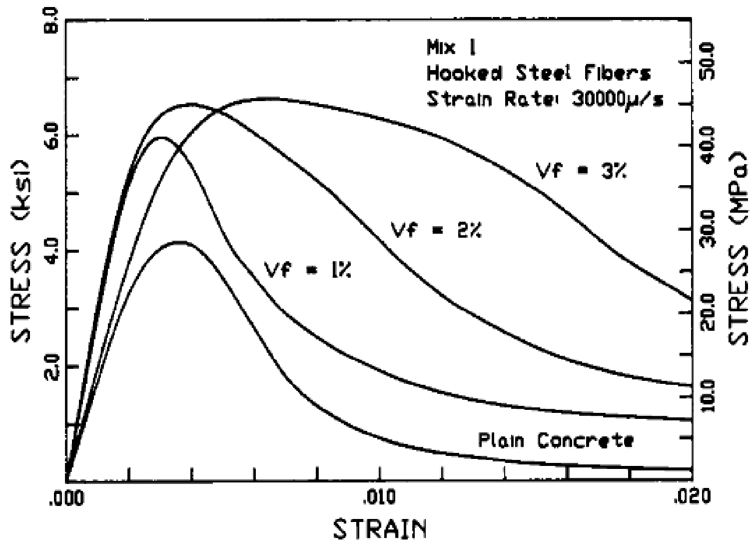

Figure 2.13 Effect of SF content on the compressive stress-strain of SFRC [55].

Singh, et al. [56] investigated the effect of SF on the compressive strength of the SFRC mixture using experimental program. Their results indicate that the addition of the SF to the concrete mix enhance the compressive strength by about 18% over plain concrete. Their experimental program containing different combinations of steel and polypropylene fibers.

2.5 Tensile strength of Steel Fiber Reinforced Concrete

Plain concrete loses their tensile load-carrying capacity almost immediately after formation of the first crack, as shown in Figure 2.16. The addition of SF to concrete mix results in significant improvement in strength of SFRC in direct tension, with increases of about 30-40% for the addition of 1-1.5% by volume of SF in concrete mix [34, 57-59]. The toughness of SFRC in tension has been improved due to addition of SF, primarily because of the large frictional and fiber bending energy developed during fiber pullout on either side of a crack, and because of deformation at multiple cracks when they occur [60, 61]. While the tensile strength beyond the first carking are not improved. Thus, SFRC is considered a quasi-brittle material with tension softening.

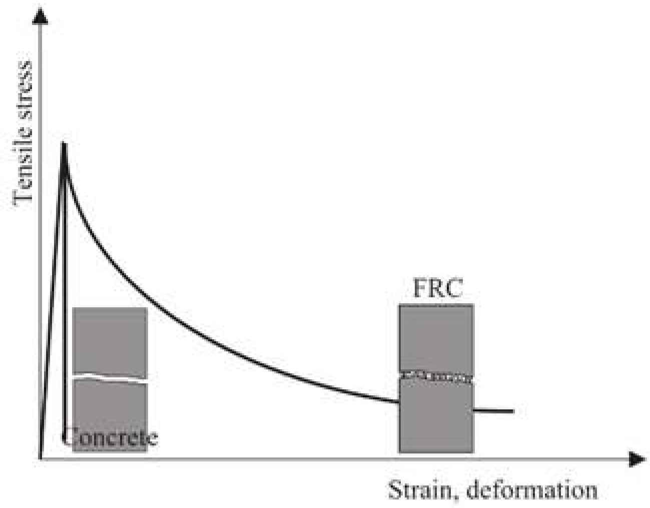

Figure 2.14 Tensile stress-strain behavior for plain and fiber concrete mixture.

The experimental assessment of the tensile properties of SFRC is difficult, and there is no standard test exists[10]. This is because, the observed experimental curve depends on the size of the specimen, that need for specimens that have a large cross section such that a fiber distribution similar to that in real structural members. Therefore, direct tensile test results are usually significantly scattered and rare. Typical stress-strain curves for SFRC in tension are shown in Figure 2.15.

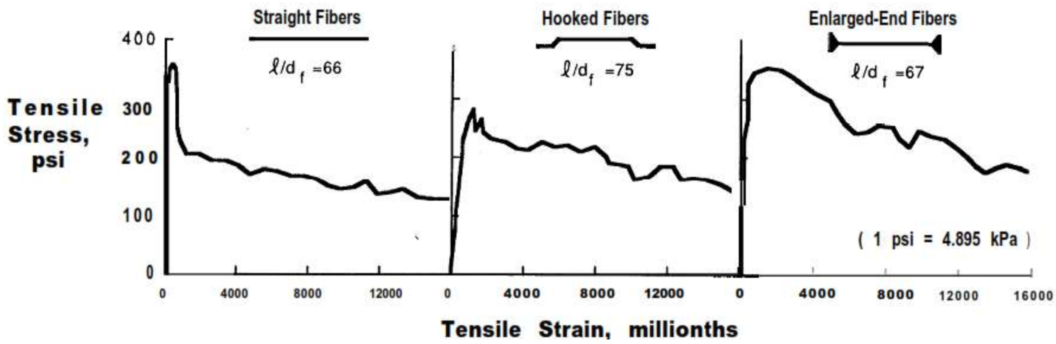

Figure 2.15 Tensile stress-strain curves for SF reinforced mortars [62]

From these experimental curves result from direct tension test performed by Shah [62], one can observe that, for the same fiber content (1.73% fibers by volume) the ascending part of the curve up to first cracking is similar to that of unreinforced mortar. The descending part depends on the fiber reinforcing parameters, particularly fiber shape, fiber amount and aspect ratio. In his research work, he presented the primary benefits of fiber addition to concrete which improve the tensile response after cracking and improve crack control. He also showed that any addition of fiber to concrete, regardless the material of fibers, type and properties of fiber, improves the tensile toughness of concrete.

Swamy and Al-Ta'an [63] present extensive experimental data to study the effect of adding SF on the behavior of SFRC, they stated that SF improves the tensile and stiffness of the concrete mix.

Shaaban and Gesund [64] carried out splitting tensile tests with 15×30cm specimens and the fiber were used 2.5 cm long corrugated SF with a tensile strength of 1240 MPa. The percentages of fibers used were 0, 4, 6, and 8 percent by weight, using rodding technique external vibrator to prepare the samples.

Yao et al. [65] investigated the mechanical properties of SFRC with 0.5% fiber volume fraction. The SF had hooked end and where 3.0 cm in length. They found that the addition of SF increases spilt tensile strength about 36.5% in comparison with unreinforced concrete.

2.6 Flexural strength of Steel Fiber Reinforced Concrete

Flexural strength of FRC can be calculated according to ASTM C78 [66], C1018-97 [67], and C1609-06 [68] by the third point loading test. Maximum flexural strength is determined at the first peak load as that value of load corresponding to the first point on the load-deflection curve where the slope is zero, that is, the load is a local maximum value.

ASTM C1018 [67] provides method for evaluating the toughness of fiber reinforced composites through the use of a toughness index. The toughness index is calculated as the area under the load-deflection curve up to the prescribed service deflection divided by the area under the load-deflection curve up to the first cracking deflection. Three indexes are described in ASTM C1018: I_s, I_{1o} and I_{20} corresponding respectively to deflections of 3, 5.5 and 10.5 times the deflection at first cracking. These indices provide indications of the shape of the load-deflection response (post cracking) and available ductility. Figure 2.16 below show ASTM C1018

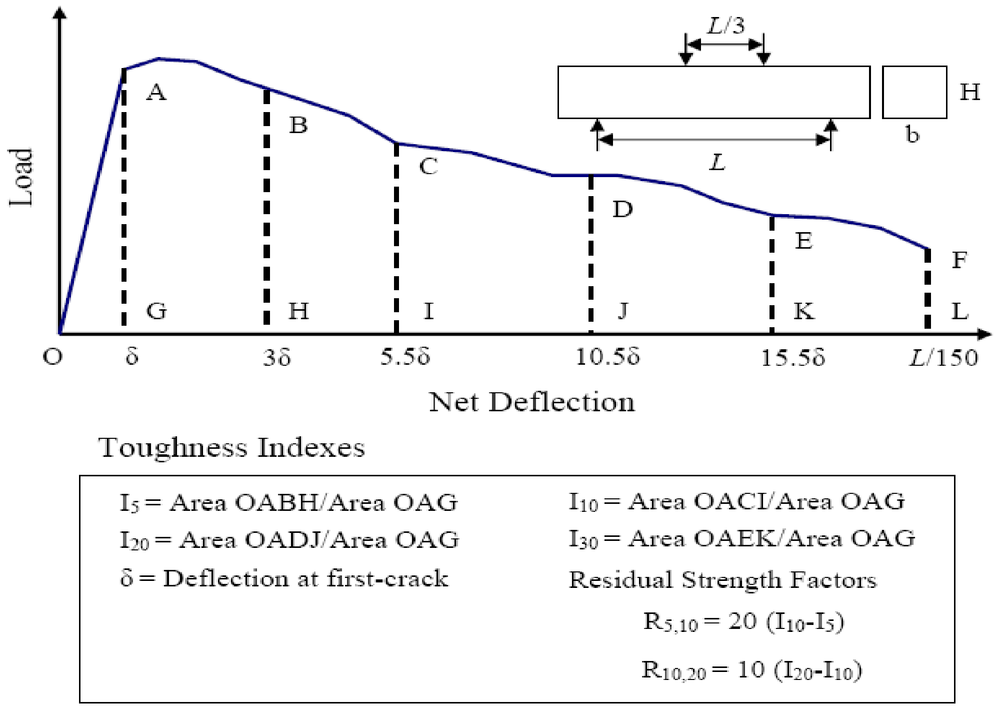

Figure 2.16 ASTM C1018 Techniques of fiber reinforced toughness characterization.

Swamy and and co-workers [69, 70] developed design equation to find the flexural strength for FRC mixture, this equation based on his effective spacing equation for FRC mixture. This equation (i.e., effective spacing equation) shows unique relationships between fiber spacing and flexural which can be divided into two stages. The first stage is the first cracking load stage in the load-deflection diagram, while the second stage is the ultimate load stage. The first crack composite flexural strength (σ_f) is:

$$\sigma_c = 0.843\ \sigma_m\ (1- V_f) + 2.00\ Vf\ (l/d) \qquad (2.1)$$

On the other head, the ultimate load stage of flexural strength (σ_{cu}) can be determine by :

$$\sigma_{cu} = 0.97\ \sigma_m\ (1- Vf) + 2.00\ Vf\ (l/d) \qquad (2.2)$$

where σ_c and σ_{cu} refer to the stress in the composite and the modulus of rupture of plain concrete respectively. Thus if the fiber geometry *(l/d)* and the fiber volume (V_f) are known, the design values of flexural strength can be directly obtained.

Stevens et al. [71] calculated the toughness index according to ASTM C1018 procedure and based on these results the following observations were made:

- Increase in fiber content results in consistent increase in ductility and energy-absorption capacity.
- Toughness Indexes 5 and 10 computed using the ASTM procedure are not sensitive enough to show the variations that are present in the load-deflection responses.
- Higher fiber contents result in much higher load-retaining capacity at large deflections.

Banthia and Trottier [72] reported that measuring true specimen deflection at first cracking, which is very important to identify toughness indexes, is difficult due to seating or the downward movement of the specimen.

Lok and Xiao [73] presented the relationship between a tensile stress-strain curves and moment-curvature behavior of SFRC. In their work, they distinguish the softening behavior from the hardening behavior of SFRC; “idealized as elastoplastic response”. They observed a notable increase in performance of SFRC in its hardened state. In addition, an increase in the tensile strength and ductility of the SFRC is evident, and they found that SFRC has beneficial flexural performance.

Abdul-Ahad and Aziz [74] studied experimentally the ultimate strength of reinforced concrete T-beams reinforced with conventional steel bars and short SF, they found that, adding the SF reduced effectively the defection, cracks width and also improved the ductility and flexural rigidity of the concrete beams. They found that a negligible difference in moment capacity between over-reinforced and under-reinforced concrete beams resulted from adding SF. Therefore, the presence of SF lead to design beams that is more economical.

Yang, et al. [75] examined experimentally the behavior of ultra-high strength concrete beams reinforced with SF. The SF ratio 2% .Their experimental test results showed that an improvement in the flexural behavior of the SF reinforced ultra-high strength concrete. Padmarajaiah, and Ramaswamy**,** [76] tested eight fully pre-stressed beams and seven partially pre-stressed beams made with high strength fiber-reinforced concrete. The volume fraction of the steel fibers ranging from 0% to 1.5% and the different location of SF in the beam.

Fu et al. [77] tested experimentally 10 specimens of SFRC; the objective of their work is to validate the positive effect of SF in crack-resistant and the flexural strength improvement of SFRC beam. Their conclusions are, the presence of SF increased the flexural strength of SFRC with concrete strength and interface transition region. Because of the existence of SF, crack-spreading path in concrete became much long and the SF with aggregate acted on crack interesting.

2.7 Shear strength of Steel Fiber Reinforced Concrete

SF increases the shear strength of concrete, the increase in shear strength for SFRC with about 1% by volume of SF is range from negligible to 30% [3, 57, 71, 78]. ACI Committee 544 report [10] present the effect of SF as relationship (see Figure 2.16), between the shear strength, the shear span-to-depth ratio (a/d), and SF content for SFRC beams from several published investigations.

They are two types of research conducted for the past four decades to study the shear behavior of SFRC beams, analytical and experimental research. Concerning the analytical research on the shear behavior of SFRC beams the same existing theories for reinforced concrete members are used and there is no significant advances have been made beyond these theories [6, 10].

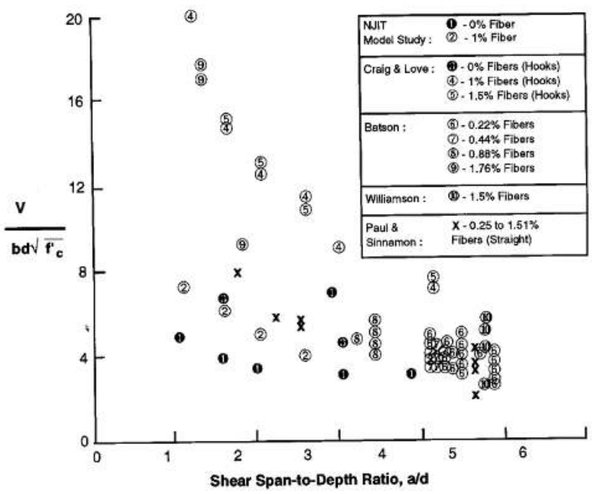

Figure 2.17 Shear behavior of reinforced SFRC beams [10].

The other type of research, experimental research has been used for the past four decades. Most of these test programs have investigated key parameters known to affect shear behavior, including shear span-to-effective depth ratio, longitudinal reinforcement ratio, SF content, type of SF and concrete compressive strength. This section presents the results of some of the research dealing with the effect of SF on shear strength in SFRC beams

Swaddiwudhipong and Shanmugam [79] reported experimental program of SFRC deep beams with openings and they studied the effect of fiber content, positions of openings, and different types of loadings on the shear behavior of these beams. Their conclusion is that SF are effective in providing extra shear strength to deep reinforced concrete beams.

Tan et al. [80] tested six simply supported I-beams under two-point loading. The SF content used is 0, 0.5, 075, 1%, with three shear span-to-effective depth ratio (1.5, 2.0, and 2.5). They found the following conclusions, the shear strength of concrete beams can be increased significantly by incorporating small quantities of SF. At a given load, the steel strains are less for SFRC beams when compared to those of RC beams, especially after diagonal cracking of the web.

Majdzadeh, et al. [81], present direct shear experimental program on SFRC specimens, they mentioned that, a linear increase in shear strength of SFRC composite is noted with the increasing the SF content. They found that, the optimal SF content is 1%,which lead to enhance the shear strength in addition to the shear toughness (energy absorption capacity) by calculated the area under the load-deflection curve for direct shear tests.

Sahoo, and Chao [82] developed an experimental program on two reinforced concrete deep beam with large single opening. The first one is reinforced concrete beam and the second one SFRC beam. They tested under monotonically increased load. The following conclusion are drawn from their work, the addition of SF in the SFRC specimen restrained the widening of crack growth and increased the number of shear cracks.

Shah, and Ribakov [83] carried out experimental program on SFRC mixture for high strength concrete to study the effect of SF on the shear behavior. They mentioned that, the low steel fiber contents (0 and 20 kg/m3)in the specimens lead to shear or compression failure type, while for specimens with steel fiber content of 40 kg/m and higher primary compression failure. Their observation concerning the addition of SF is lead to the improvement in the ductility, toughness, flexural strength, and shear strength of SFRC.

Zhang, et al [84] develop an experiment test program including two large-scale rectangular hollow pier specimens, with small amounts of transverse reinforcement. They made a finite element analysis and compare the numerical results with those obtained from their experimental results. Based on their parametric study of SF content, they observed that, shear strength in addition to the flexural strength, ductility and energy dissipation of the hollow piers are improved with the increase of steel fiber content, up to 1.5% fiber volume ratio. Their observation reach that, the addition of SF volume ratio by about 1.0% to hollow SFRC members under test preformed similarly to reinforced concrete members having 2.6 times more shear steel. Thus, one can reach to the use of SFRC can substitute part of the shear reinforcement in hollow piers.

Arslan [85] develop a design expression for the shear strength of SFRC beams. His proposed equation and researchers' predictions are compared to the test results of 170 SFRC beams without stirrups. The analytical models to predict the shear strength for SFRC beam without stirrups considered in his study are presented in Table 2.4

He concluded that, the proposed equation has the lowest coefficient of variation in Table 2.4, and hence provides better results than the eleven different methods for the prediction of shear strength of SFRC beams. So one who interested in analytical shear strength prediction can make use of Table 2.4 and reference [85] to find the state of the art articles concerning analytical shear strength prediction for SFRC beams.

Simasathien and Chao, [86] investigate the shear behavior of deep SFRC hollow-core slabs, with a depth of 460 mm. Based on their experimental program, that ultimate shear strengths for hollow-core slab with 0.75% SF by volume slab are approximately twice those without using SF. They conclude that, SFRC is more efficient in hollow-core slabs than in typical beams the efficiency of the fiber-bridging effect, which is greater when fibers are used in hollow-core slabs than in beams. They stated that, the increase is due to the thin webs of the hollow-core sections, which lead to the preferable fiber orientation along the axis of the slabs. Their recommendation is, the fiber length should be at least 80% “to ensure a preferred fiber orientation” of the thickness of the web of the hollow-core units, with an aspect ratio between 50 and 100 “to maintain workability of the concrete”.

Table 2.1 Existing shear strength models for SFRC beams without stirrups [85]

Reference	Shear strength models (MPa)
Sharma (1986)	$v_u = kf_t(d/a)^{0.25}$ $k = 1$ and 2/3 for direct and indirect tension tests, respectively; $k = 4/9$ if f_t is obtained using modulus of rupture; or $f_t = 0.79f_c^{0.5}$
Narayanan and Darwish (1987)	$v_u = e[0.24f_{sp} + 80\rho d/a] + v_b$, $f_{sp} = f_{cuf}/(20-\sqrt{F}) + 0.7 + 1.0\sqrt{F}$ $v_b = 0.41\tau F$, $e = 1$ for $a/d > 2.8$, $e = 2.8\, d/a$ for $a/d \leq 2.8$ $d_f = 0.5$ for round, 0.75 for crimped, 1.0 for indented fibers.
Ashour *et al.* (1992)	$v_u = (2.11f_c^{1/3} + 7F)(\rho d/a)^{1/3}$ for $(a/d) \geq 2.5$
Swamy *et al.* (1993)	$v_u = 0.37\tau V_f L_f/D_f + 0.167\sqrt{f_c}$
Imam *et al.* (1997)	$v_u = 0.6\frac{1+\sqrt{(5.08/d_a)}}{\sqrt{1+d/(25d_a)}}\sqrt[3]{\rho(1+4F)}\left[f_c^{0.44} + 275\sqrt{\frac{\rho(1+4F)}{(a/d)^5}}\right]$ $d_f = 0.50$ for smooth, 0.9 for deformed, 1.0 for hooked fibers.
Khuntia *et al.* (1999)	$v_u = (0.167 + 0.25F)\sqrt{f_c}$ $d_f = 2/3$ for plain and round, 1.0 for hooked or crimped fibers.
Kwak *et al.* (2002)	$v_u = 2.1ef_{sp}^{0.7}(\rho d/a)^{0.22} + 0.8(0.41\tau F)^{0.97}$ $e = 1$ for $a/d > 3.5$; $e = 3.5d/a$ for $a/d \leq 3.5$
RILEM (2003)	$v_{Rd,3} = v_{cd} + v_{fd}, v_{cd} = 0.12k(100\rho f_c)^{1/3}, k = (1+\sqrt{200/d}) \leq 2, \rho \leq 0.02$, $v_{fd} = 0.7k_f\, k_l\, \tau_{fd}, k_1 = (1600-d)/1000 \geq 1, \tau_{fd} = 0.12f_{eqk,3}$, $f_{eqk,3}$= characteristic value of the equivalent tensile strength, $k_f = 1$ for rectangular sections
Yakoub (2011)	$v_u = \beta\sqrt{f_c}(1 + 0.70V_f\, L_f\, d_f/D_f)$ for $a/d \geq 2.5$ $\beta = \frac{0.40}{1+1500\varepsilon_x}\frac{1300}{1000+s_{xe}}, \varepsilon_x = \frac{M/d_v + V}{2E_sA_s}s_{xe} = \frac{35s_x}{16+d_a} \geq 0.85s_x$ M and V are the external failure moment and shear acting on the section, s_x = crack spacing parameter ($\cong d_v$, flexural lever arm), $d_v = 0.9d$ or $d_v = 0.72h$, ε_x = longitudinal strain at the middepth, $d_f = 0.83$ for crimped, 0.89 for duoform, 1.00 for hooked, 0.91 for rounded fibers.
Gandomi *et al.* (2011)	$v_u = \frac{2d}{a}(\rho f_c + v_b) + \frac{d}{2a}\frac{\rho}{(288\rho - 11)^4} + 2$
Dinh *et al.* (2011)	$v_u = 0.13\rho f_y + 1.2\left(\frac{V_f}{0.0075}\right)^{1/4}\left(1-\frac{c}{d}\right), c = 0.1h$

f_{sp} = computed value of split-cylinder strength of fiber concrete; f_{cuf} = cube strength of fiber concrete; d_a = maximum aggregate size; h = beam height; F = fiber factor $(= L_f V_f d_f/D_f)$; v_u = ultimate shear strength; v_c = shear resistance of concrete, v_b = contribution of steel fibers to shear strength; τ = average interfacial bond stress of fiber matrix; τ_{fd} = design shear stress; e = arch action factor.

CHAPTER 3

EXPERIMENTAL PROGRAM

3.1 General

The aim of the study is to examine the effect of SF on the behavior of solid and hollow beams with different shear span to effective depth ratio (a/d). However, beam size, fiber type and longitudinal reinforcement ratio are left unchanged.

Experimental program of the present work is attempt to matching the both lightweight structural member with the structural ductility requirements. This can reach by combining the optimum beam's section topology with using SF reinforcement. Therefore, the investigated parameters are shear span to depth ratio (a/d) and hollow shape.

Three values for (a/d) are used for investigating 8, 6, and 4. Two hollow type of circular and square shape are considered. All these parameters are compared with the control specimens of solid and hollow sections of normal concrete.

The details of the experimental program, test specimens description, detail of reinforcement, specimen construction, and material properties are presented in this Chapter.

3.2 Test Program

Experimental program of the present work are consists of the following stages:

- Designing the beams according to ACI 318M standards.
- Preparing and casting the specimens according to the optimum SF ratio ν_f that obtained from the literature which is equal to 1.0%.
- Testing stage include, investigate the deflection due to loading history by using LVDT and strain gages for concrete.

- The results from the previous stage will compared with control specimens. in this stage the specimens are constructed using normal concrete,
- Variable shear span to depth ratio (a/d) will be used (4, 6, and 8); more over the optimum hollow area will be used with different shape (circular and square).
- The tested specimens are subject to two points load.

A test matrix, Table 3.1, is developed to study the effect of using the above different parameters on the behavior of beams. The test matrix is divided into five groups based on the variation of the above-mentioned parameters. The description of each group is presented in the following sub sections.

3.2.1 Group A

Group A consisted of two tests on two beams. The tested beams have solid cross section with longitudinal reinforcement of 2Ø8 mm. The beams have length L 2450 mm, height h 150 mm and the width b 150 mm. The effective depth of the beam d is equal to 125mm and concrete cover is 25 mm.

The first beam that has 0% of SF is considered to be the control beam, while the second beam is with SF 1.0%. Concrete compressive strength, beam size, fiber type and longitudinal reinforcement ratio are left unchanged. The beams are designed to fail due to flexural failure prior to the shear failure. The tested specimen details are shown in Figure 3.1.

A control beam without transverse reinforcement (i.e. stirrups) was tested to compare the results with the beams that had only SF. Thus, the objective of this group is to study the effect and the behavior of the SFRC beam without shear reinforcement.

Table 3.1 Present test program matrix

Group	Beam cross-section	(a/d) ratios	Stirrups	SF ratio	Name
A	solid section	8	φ5.3@1.2 = 3	zero	N-L8-0-3
				1.0%	S1-L8-0-3
B	solid section	8	φ5.3@75 = 32	zero	N-L8-0-32
	Square Hollow type 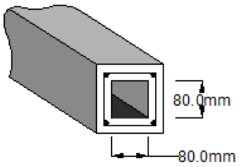	8	φ5.3@75 = 32	zero	N-L8-80-32
	Circular Hollow type 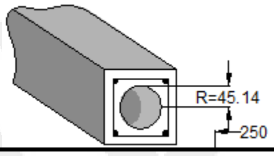	8	φ5.3@75 = 32	zero	N-L8-C80-32
C	solid section	8	φ5.3@75 = 32	1.0%	S1-L8-0-32
	Square Hollow type 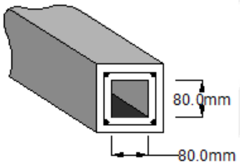	8	φ5.3@75 = 32	1.0%	S1-L8-80-32
	Circular Hollow type 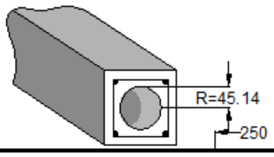	8	φ5.3@75 = 32	1.0%	S1-L8-C80-32
D	Square Hollow type 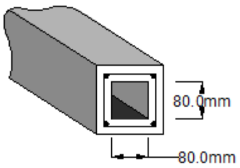	6	φ5.3@75 = 24	1.0%	S1-L6-80-24
		4	φ5.3@75 = 18	1.0%	S1-L4-80-18
E	Circular Hollow type 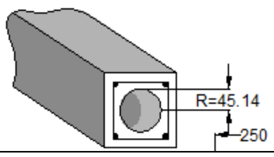	6	φ5.3@75 = 24	1.0%	S1-L6-C80-24
		4	φ5.3@75 = 18	1.0%	S1-L4-C80-18
N: Normal Concrete SX: SF ratio (Ex S1 1 % SF): 80: Refer to square hollow size, C: Refer to that circle radius equivalent to square and L8: L refer to L1 , 8 refer to L1/ d					

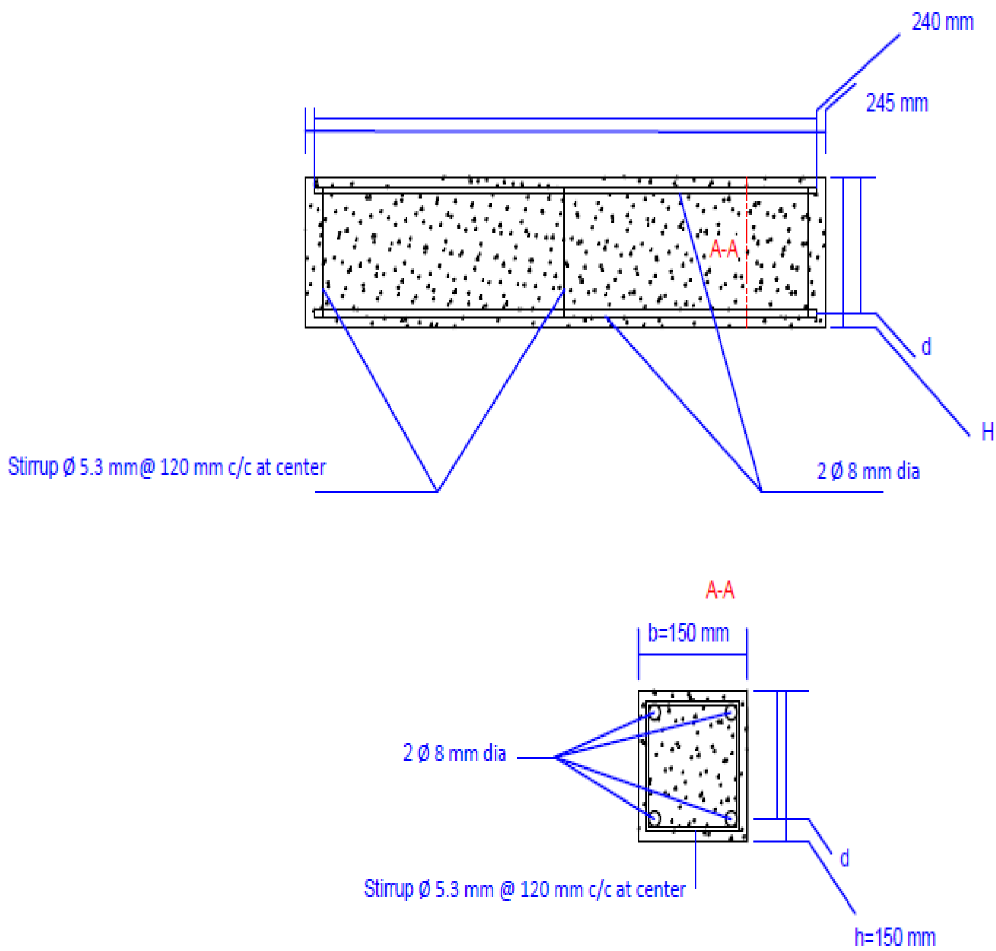

Figure 3.1 Details of beam specimens of Group A

3.2.2 Group B

Group B consisted of three tests on three beams. The tested beams have solid cross section with square hollow cross section and circular hollow cross section with longitudinal reinforcement of 2Ø8 mm. The length of beam L is equal to 2450 mm, height h is 150 mm and the width b is 150 mm. The effective depth of the beam d is equal to 125mm and. concrete cover is equal to 25 mm. The all beams transverse reinforcement and without SF (0.0%). The beams are designed to fail due to flexural failure prior to the shear failure. The tested specimen details are shown in Figure 3.2.

A control beam solid cross section was tested to compare the results with the beams that had square hollow with circular hollow. The objective of this group is to study the effect and the behavior of the hollow cross section type's concrete beam without SF.

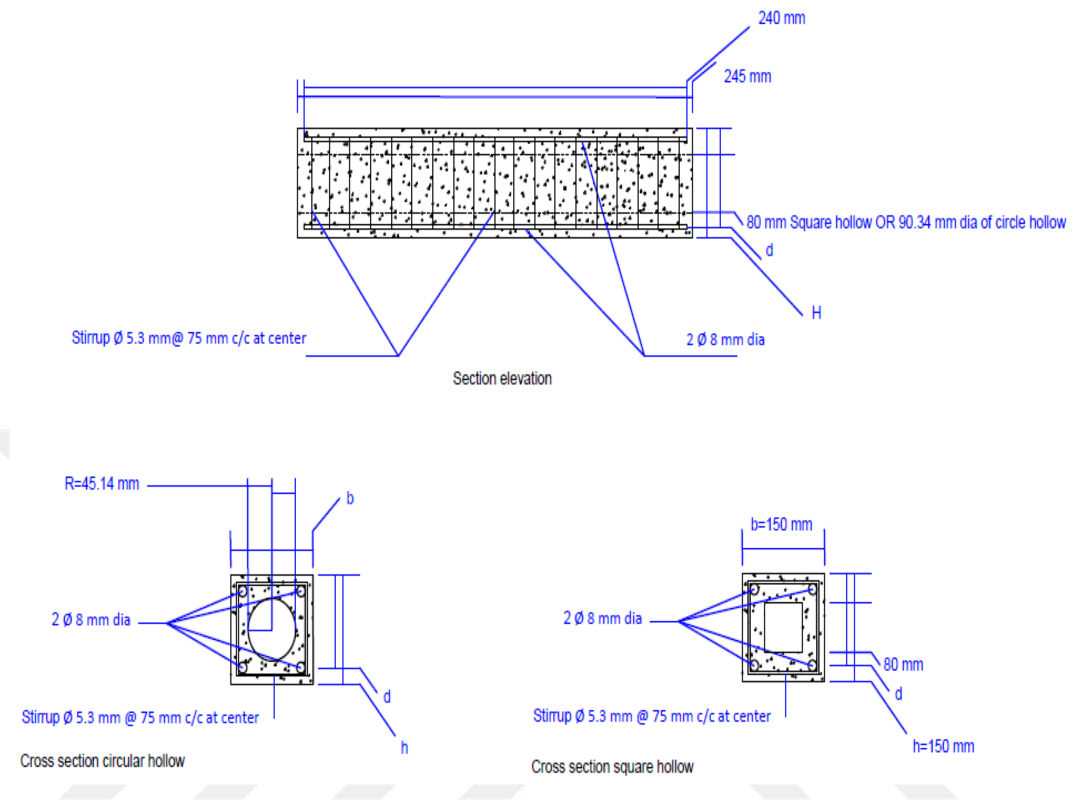

Figure 3.2 Details of beam specimens of Group B.

3.2.3 Group C

Group C consisted of three tests on three beams. The tested beams have solid cross section with square hollow cross section and circular hollow cross section. The beams have length L 2450 mm, height h 150 mm and the width b 150 mm. The effective depth of the beam d is equal to 125mm and concrete cover is equal to 25 mm. The all beams transverse reinforcement and with SF (1.0 %). The tested specimen details are shown in Figure (3.3).

A control beam solid cross section was tested to compare the results with the beams that had square hollow with circular hollow. The objective of this group is to study the effect and the behavior of the hollow cross section type's concrete beam with SF.

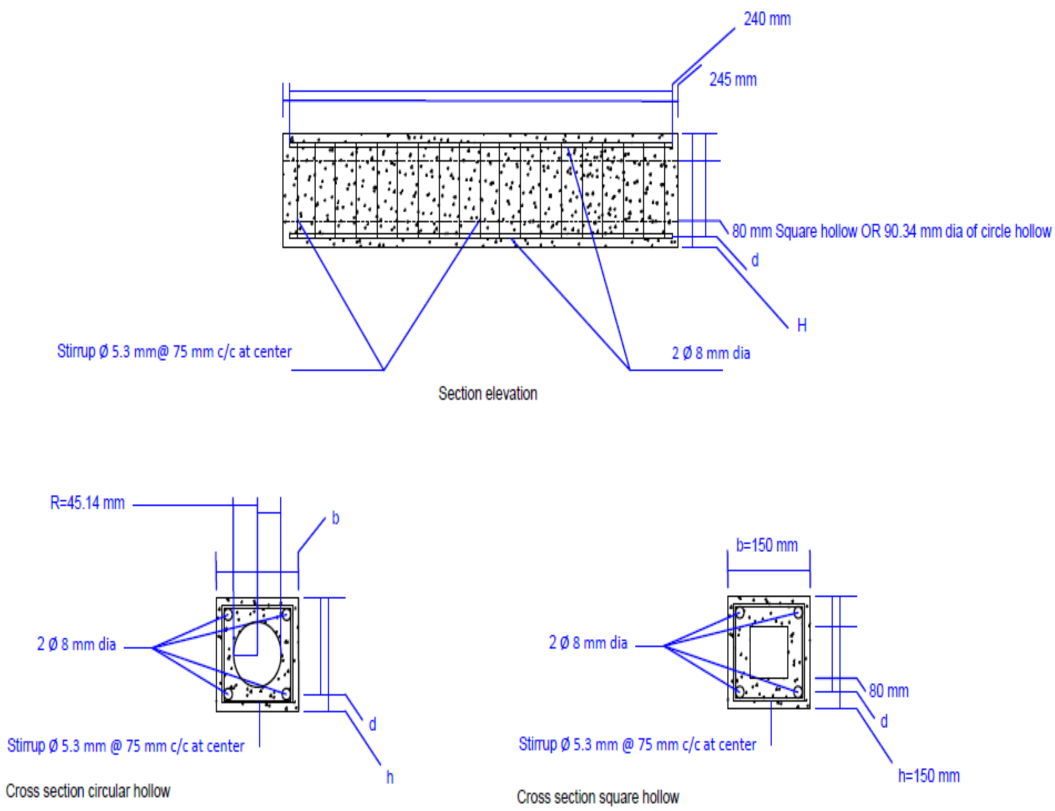

Figure 3.3 Details of beam specimens of Group C.

3.2.4 Group D

Group D consisted of two tests on two beams. The tested beams have square type hollow cross section. The height of beam h is equal to 150 mm and the width b is equal to 150 mm. The effective depth of the beam d is equal to 125mm and concrete cover is 25 mm. The first beam that has length L 1900 mm which is considered to be the control beam, while the second beam length is 1400 mm.

The all beams transverse reinforcement and with SF (1.0 %). Concrete compressive strength, beam size, fiber type and longitudinal reinforcement ratio are left unchanged. The tested specimen details are shown in Figure 3.4.

A control beam square hollow cross section was tested to compare the results with the beam that had square hollow with different longitudinal reinforcement. The objective of this group is to study the effect and the behavior of the square hollow cross-section type

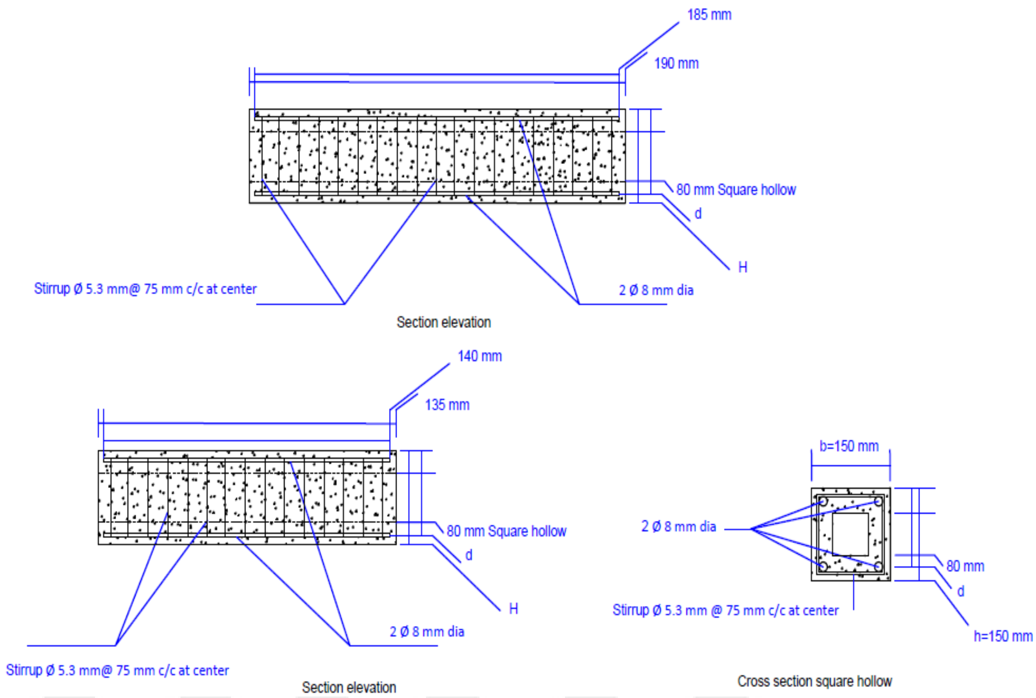

Figure 3.4 Details of beam specimens of Group D

3.2.5 Group E

Group E consisted of two tests on two beams. . The tested beams have circular type hollow cross section. The height of beam h is equal to 150 mm and the width b is equal to 150 mm. The effective depth of the beam d is equal to 125mm and concrete cover is 25 mm. The first beam that has length L 1900 mm which is considered to be the control beam, while the second beam length is 1400 mm.

The all beams have SF (1.0%). Concrete compressive strength, beam size, fiber type and longitudinal reinforcement ratio are left unchanged. The tested specimen details are shown in Figure 3.5.

A control beam circular hollow cross section was tested to compare the results with the beam that had circular hollow. The objective of this group is to study the effect and the behavior of the circular hollow cross section type concrete beam.

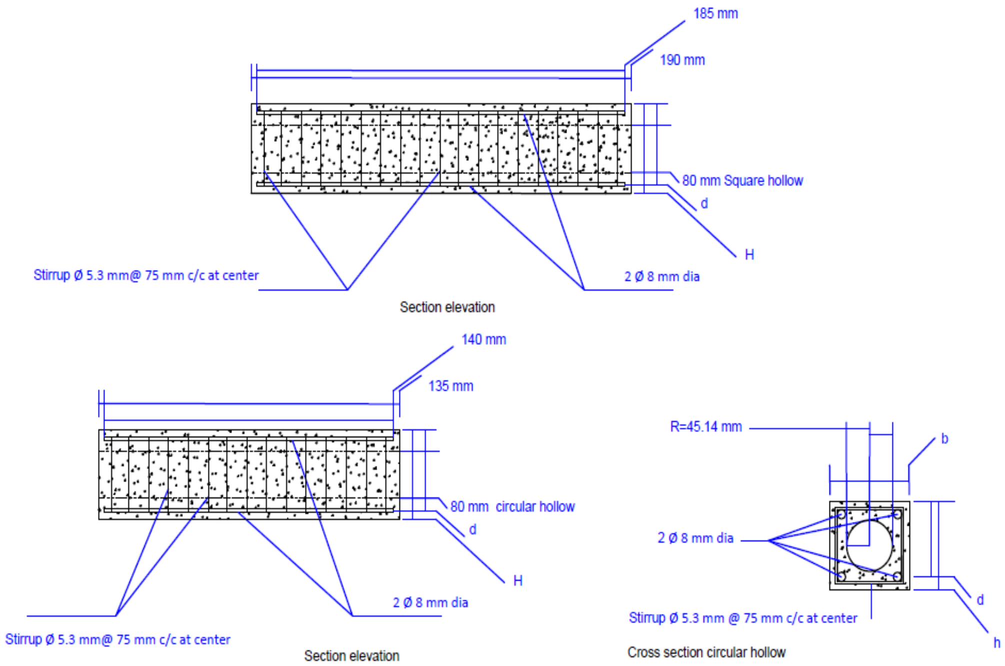

Figure 3.5 Details of beam specimens of Group E

3.3 Specimen Details

The test specimen was reinforced concrete beam with length of L 2450 mm, 1900 mm and 1400mm. The height of all beams h 150mm and the width b 150mm. The effective depth of the beam d is equal to 125mm and concrete cover is 25 mm. Beams have different cross section (such as solid, square hollow, circular hollow) The dimension of square hollow 80×80mm and circular equivalent to box space .

3.2.6 Steel detail

The longitudinal reinforcement bars are 2Ø8 mm, with two tie bars at the top and two flexural bottom bars. The shear reinforcement (stirrups) is Ø5.3 @75mm c/c.

3.2.6.1 Test specimens without stirrups

Test specimens without stirrups consisted of two beams and named as group A. The test specimens have solid cross section with longitudinal reinforcement. The length of beam L is equal to 2450 mm. The first beam that has 0% of SF is considered to be the control beam, while the second beam with SF 1.0%. Figure 3.6 shows test specimen without stirrups.

Figure 3.6 Fabrication of specimens of Group A.

3.2.6.2 Test specimens with stirrups

Test specimens with stirrups consisted of four group of beams which are Groups B, C, D and E. The test specimens have solid, square hollow and circular hollow cross section with longitudinal reinforcement. The fabrication of solid and hollow beam (Groups B, C, D and E) with shear reinforcement (stirrups) are shown in Figure 3.7 and Figure 3.8 respectively.

Figure 3.7 Fabrication of specimens with stirrups.

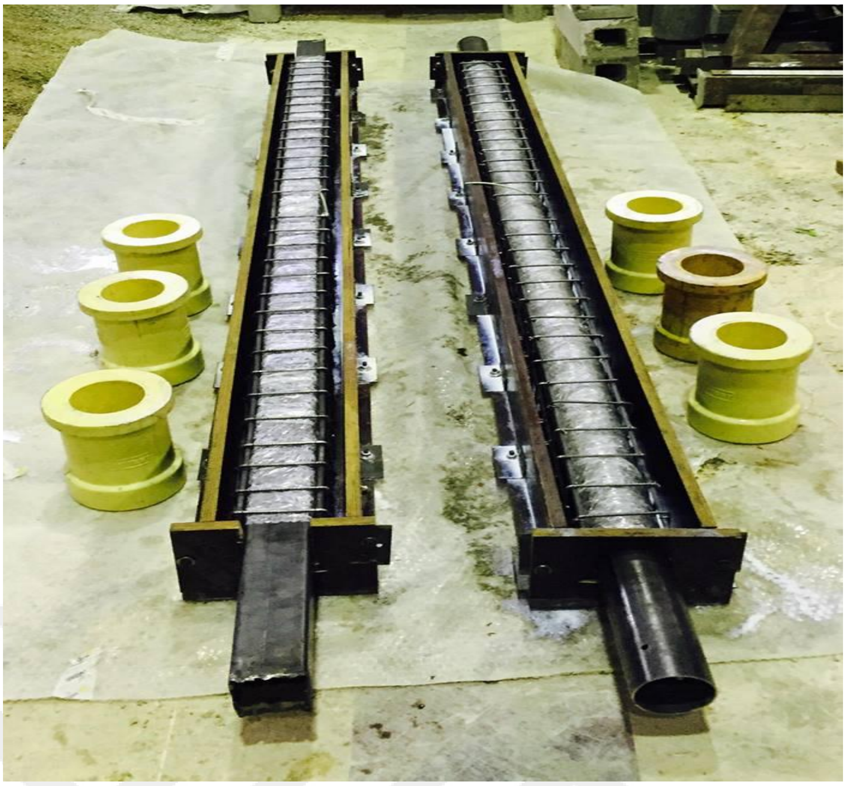

Figure 3.8 Fabrication process of hollow specimens with stirrups.

3.3 Specimen Fabrication

As stated above, all beams were designed a solid and hollow beams. They are constructed (casted) at the University of Gaziantep Structural Engineering Laboratory.

3.3.1 Mix Design

The result of the mix design are given in the Table 3.2.

Table 3.2 Mix design used in the present study

Mix design code	SF	Cement (kg)	Gravel (kg)	Sand (kg)	Silica füme (kg)	HWR (kg)	Water (Lt)
N	0.0%	465	680	1170	35	6.6	216
S1	1.0%	465	630	1170	35	6.6	216

3.3.2 Mixing Procedure

The mixing materials are added in the mixer machine and blended according to a certain speed for the required period. To be added all the materials mentioned in Table 3.2 and stays blending machine to work to see that the mixing of materials was excellently stop blending machine and then made the casting process in the beam mold. The mixer procedure is shown in Figure 3.9.

Figure 3.9 Mixer procedure

3.3.3 Casting and curing procedure

After mixing of materials of concrete blending well by mixer machine. The concrete paste are taken and concrete are poured into the molded. Before casting process mold painted with oil and placed steel reinforcement in the mold. In order to reach the full casting, vibrator is used during the molding process. As for the ripening process of concrete is up model that has been poured filer a cloth absorbs water and holds it for a period of curing. The curing process takes a period of 28 days. Figures 3.10 - 3.11 show the casting and curing process.

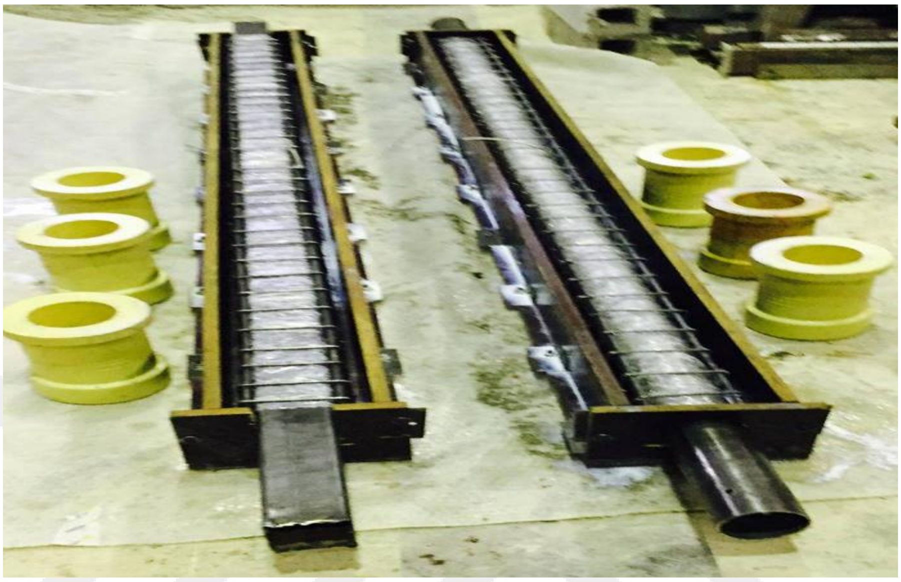

Figure 3.10 Molding process.

Figure 3.11 Casting process.

Figure 3.12 Final casting and vibrating stage.

Figure 3.13 Curing process.

3.4 Material Properties

3.4.1 Steel reinforcement

The longitudinal steel reinforcement was diameter Ø8 mm deformed bars with nominal yield strength of fy 579 MPa. The shear reinforcement used in the test region was plain bars with measured yield strength of fy=400MPa and a diameter of Ø5.3 mm. the properties of steel reinforcement used in the present study presented in Table (3.3)

Table 3.3 Properties of steel reinforcement used in present study

Nominal Diameter Size (mm)	Cross section area (mm^2)	Weight (Kg/m)	Yield Stress (fy) (Mpa)	Ultimate Stress (fu) (Mpa)
8	50.3	0.395	579	648
5.3	19.60	0.15	400	450

3.4.2 Steel fiber

The type of SF used which is hooked end (cold drawn wire) classes defined by (ASTM A820) is shown in Figure 3.14. The specifications for the SF presented in Table 3.4.

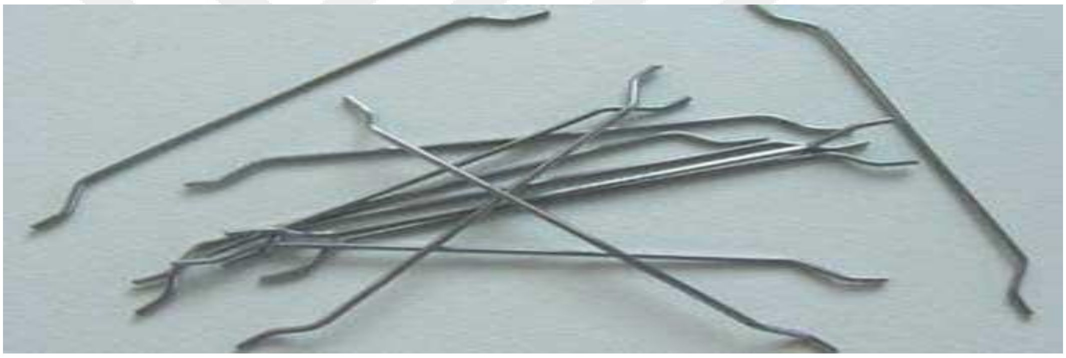

Figure 3.14 Hooked ended SF used in the present study.

Table 3.4 Properties of SF used in present study.

L [mm]	D [mm]	L/D	fy [N/mm^2]	Number of SF/kg	Density kg/m3
30	0.55	54.55	1500	16750	7850

3.4.3 Cement (PC)

The type used in the present work is Portland cement type (CEM ll / A-LL 42.5 R). The chemical and mechanical properties are listed in Tables (3.5) and (3.6) respectively.

Table 3.5 Chemical compositions of Portland cement

Analysis Report (%)	**Cement**
CaO	63.79
SiO_2	20.03
Al_2O_3	4.03
Fe_2O_3	2.59
MgO	2.96
SO_3	2.76
K_2O	0.71
Na2O	0.10
MnO	2.06
Ignition loss	6.13
Specific surface area (m^2/kg)	326
Specific gravity	3.15

Table 3.6 Physical and mechanical properties of Portland cement

Compressive strength at 28 day (MPa)		**Initial setting time (min)**	**Soundness expansion (mm)**
Minimum	Maximum	≥60	≤10
42.5	62.5		

3.4.4 Coarse and fine aggregate

Crushed stone with a maximum size of 4 mm was used in this experiment as course aggregate. The fine aggregate which is natural river sand and has maximum size of 0.5 mm is utilized in this research. The aggregates are shown in the Figure 3.15. Sieve analysis of fine and course aggregates are given in Table 3.7

(a) (b)

Figure 3.15 Aggregates, (a) coarse aggregate (b) fine aggregate

Table 3.7 Sieve analysis of fine and course aggregates

Sieve Size (mm)	**Crushed stone 16-8 mm**	**Crushed stone 8-4 mm**	**Natural Rivers and 0.5 mm**
0.25	0	0	3.79
0.5	0	0	14.27
1	0	0	30.85
2	0	0	49.35
4	0	2.05	83.06
8	1.28	66.66	100
16	78.19	100	100
Specific gravity	2.66	2.65	2.58

3.4.5 Silica fume

In Current search, silica fume was used as additional cementations material. Specific gravity and specific surface area of the silica fume were 2.2 and 21.80 m^2/kg, respectively. The properties of silica fume is given in Table 3.8.

Table 3.8 Properties of silica fume

Constituent (%)	Silica Fume
Ca O	0.45
SiO	90.36
Al2O3	0.71
FeO3	1.31
SO3	0.41
K2O	1.52
Na2O	0.45
Loss of Ignition	3.11
Specific Surface	21. 80
Specific Gravity	2.2

3.4.6 Water

The tap water has been used for both mixing and curing of concrete.

3.4.7 Mineral admixture

Master Gallium® 51 is used in present study. Consistent with the TS EN 934-2 high range water reducing/super plasticizer concrete admixture and ASTM C494 Type F. The specific gravity of 1.07 was utilized every concrete mixes. The detailed characteristics of used high range water reducing admixture. The properties of mineral admixture is given Table 3.9.

Table 3.9 High range water reducing admixture

Properties	HRWRA
Name	Glenium 51
Color	Dark brown
Condition	Liquid
Specific gravity (kg/l)	1.07
Chemical description	Modified polycarboxylic ploymer
Recommended dosage	1-2% (% binder content)

3.5 Mechanical Properties

3.5.1 Fresh Properties - Slump Test:

The fresh properties of FRC mixtures were evaluated with slump testing. According ASTM C 143 for the slump test. The slump test was performed on concrete with and without fiber during the mixing procedure to compare the fibers effect on workability. Figure 3.16 shows the slump test measurement.

3.5.2 Hardened concrete test

3.5.2.1 Compressive strength test:

According ASTM C39/C39M-12a, compressive strength used for conventional concrete can be used FRC. Cylinders have been tested in both the normal and SF. And made a capping cylinders of sulfur material for each cylinder according ASTM C617 and then the test. Cylinder is placed in a compressive test machine and a constant load is applied to the cylinder until it breaks. Building Materials Testing Systems CODE:BCO-IS SERIES . Figure 3.17 compressive machine test and test specimens.

Figure 3.16 Slump test measurement.

Figure 3.17 Compressive test machine.

3.5.2.2 Indirect tensile test:

According ASTM C496 spilt cylinder testing. Used for conventional concrete can be used FRC. Cylinders have been tested in both the normal and SF. Cylinder is placed in indirect tensile test machine and a constant load is applied to the cylinder until it split. Building Materials Testing Systems CODE:BCO-IS SERIES. Figure 3.18 shows indirect tensile testing of specimen.

Figure 3.18 Indirect tensile test machine

3.6 Testing Detail

3.6.1 Test Setup of Beam

The beam has been prepared for the test. The beams are placed one next to the other as shown in Figure 3.19 and are painted one side which is used for observation of crack during test.

Figure 3.19 painting and meshing process of beam specimens

3.6.2 Instrumentation

A device named (INSTRON FLEXURAL TEST) is used for the beam test. The test machine has high specification. The 5980 Series, manufactured by Instron®, is a floor model universal testing systems for high-capacity testing up to 600 kN re universal. It has a static testing system that performs tensile and compression testing as well as shear, flexure, peel, tear, cyclic, and bend tests. It is designed to guarantee a precise, durable and versatile function for the modified necessity. It has an option of basic features that develops the efficiency in testing and enhance the testing experience for the operators. It comes with a wide variety of frames that are accessible that can hold a capacity of 100, 150, 250, 400 and 600 kN. Figure 3.20 shows Instron test machine.

Figure 3.20 Instron 5985 flexural test

3.6.3 Accessory with the device

In order to test the beams studied in this thesis, addition support system is design and produced by Abbass [91]. This support system is placed on the base device and also to raise the sampled. The manufacturing photographs are shown in Figure 3.21.

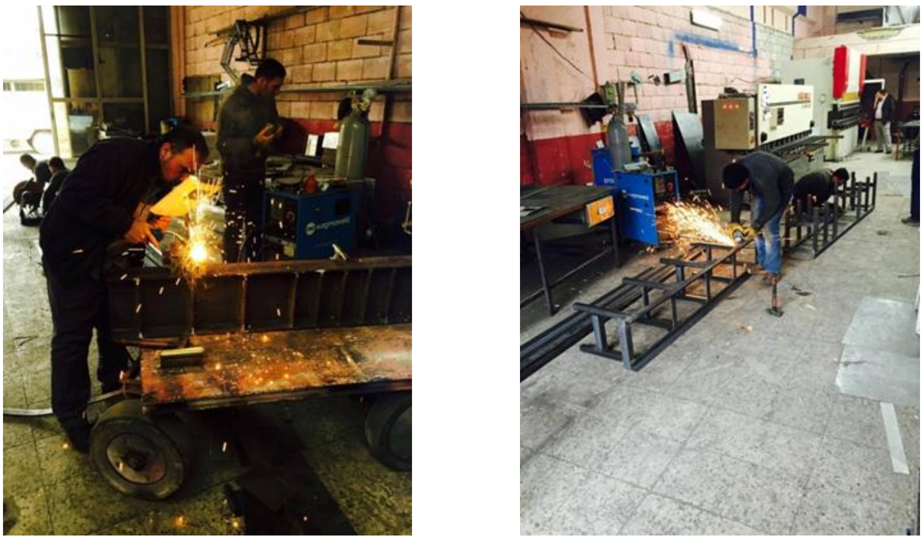

Figure 3.21 Manufacturing of support

3.6.4 Testing procedure of beam

The method of testing was done according to displacement control method, and the device was calibrated at speed (0.4 mm/min). The distance between the two point loads was kept constant at 250 mm. The vertical deflection and the strains at the top and bottom of the beam were measured. Visual observations of any cracks were made during the test and all cracks were marked. Figure 3.22 shows some specimen under test.

Figure 3.22 Beam specimens under test.

CHAPTER 4

EXPERIMENTAL PROGRAM RESULTS

4.1 Introduction

The objective of this chapter is to cover the experimental results analysis of the fresh properties (workability) and the mechanical properties (compressive strength, tensile strength, and structural behavior) of the SFRC.

In order to achieve the effect of hooked ended SF on the above-mentioned properties, 45 cylinder specimens and 12 beams were casted. The fabrication, curing of the test specimens, and test program presented in details in Chapter 3.

This chapter was divided into two parts, the first part concerning with the workability test of fresh concrete, results of compression test at test ages of 7, 28 and 90 days respectively, and indirect tensile test. While, the structural behavior of the SFRC beams under monotonic loading presented and discussed for each group in the second part.

4.2 Workability and Mechanical Properties of Steel Fiber Reinforced Concrete

4.2.1 Workability

Workability is defined as “that property of freshly mixed concrete which determines the ease and homogeneity with which it can be mixed, placed, consolidated, and finished to a homogenous condition.” [30].

The most commonly used method to measure the workability of concrete is slump test, which is specified in ASTM standard as a test method for determination of slump of hydraulic cement concrete (ASTM C143/143M) [87]. This test is the most well-known and widely used method to characterize the workability of fresh concrete, which can be used either in laboratory or at site of work.

In the present experimental work, slump test is performed on plain concrete mixture without SF termed (control specimen) and on SFRC specimen. Figure 4.1 shows the slump test performed in the present study.

Figure 4.1 Slump test performed in the present study.

The test results of fresh properties of plain concrete and SFRC with 1% volume fractions of fiber are presented in Table 4.1

Table 4.1 Slump test results of the present study.

Mix No.	***Mix Symbol***	***Standard slump test (mm)***
1	NC	103
2	1.0% SF	65
NC = Normal concrete and SF = Steel Fiber		

From Table 4.1, it is noted that when SF is added to concrete with 1% volume fractions of fiber reduce the workability of concrete. From results of Mix 1 and Mix 2, it is noted that in Mix 2 the slump decreased by 36.89%, compared with that of control mix (Mix 1). This is due to the fact that, adding SF will form a network structure in concrete mixture, which restrain concrete from segregation and flow Finally, it is concluded that the workability of concrete mixture decreases with the addition of hooked ended SF.

4.2.2 Compressive strength

The addition of fiber to the concrete mixtures has effects on the mechanical properties of hardened concrete, in this subsection, the SF effect on the compressive strength of concrete mixture is studied by casting, curing, capping, and testing of 18 cylindrical concrete specimens.

A cylinder dimension chooses for this study with a 100 mm diameter and 200 mm in high which is the more common dimensions used and to ensure a SF distribution in concrete mixture similar to that in the beam specimens. Figure 4.2 shows the cylindrical test specimens

Figure 4.2 Cylindrical specimens fabricated in the present study.

The cylinders samples are taken based on ASTM C172/C172M [88], compacted, and cured based on ASTM C31/C31M [89]. The cylinders are covered with a lid sheet and left for one day in the laboratory. Then the specimens are demolded the next day and submerged in a water tank for curing until being tested. Two days prior to the test date, the cylinders are pulled out of the water tank. The cylinders are capped as shown in Figure 4.3, based on ASTM C617/C617M [90], with a sulfur cap at the top ends, which are the two ends parallel to each other to guarantee that the specimens are subjected to a uniform axial load.

Figure 4.3 Sulfur capping of cylindrical specimens used in the present study.

The compressive strength tests are performed on plain concrete (control mix) and on SFRC mixture at the age of 7, 28 and 90 days. Then the compressive strength f_c' is calculated based on the axially applied load and the size of the cylinder specimen. Three replicated cylindrical specimens are tested for each test age. The concrete compressive strength for cylinders corresponding to plain and SF concrete are reported in Table 4.2

The compressive strength increases with age for both non-fibrous and fibrous mixes as shown in Figure 4.4. The compressive test results for the cylindrical specimens show that, the addition of SF has a slightly negative effect on the compressive strengths of concrete at early ages (7 days). This is may be due to lower bond between SF and concrete at early ages; also the addition of SF to concrete increases porosity and decreases the bond between concrete and steel in addition to the effect of the superplasticizer dosage of, which has a retardation effect. The SF mixture has higher compressive strength values than that of the reference mixture at 28, and 90 days with an incensement percentage about 48.8% and 49.4% respectively as shown in the Figure 4.4.

Table 4.2 Compressive strength results for plain and SF concrete specimens

Specimens. code	V_f (%)	***Temp.*** (°C)	***Age*** (day)	***Load*** (kN)	f'_c (MPa)	***Avg. fc*** (MPa)	***Diff*** %
HN1-7	0	20	7	245.18	31.20	31.14	
HN2-7		20	7	203.94	25.95		
HN3-7		20	7	284.90	36.26		0.93
HS1-7	1	20	7	252.19	32.09	29.24	
HS2-7		20	7	215.80	27.46		
HS3-7		20	7	221.28	28.16		
HN1-28	0	20	28	366.51	46.64	45.76	
HN2-28		20	28	330.11	42.01		
HN3-28		20	28	382.07	48.62		48.8
HS1-28	1	20	28	532.42	67.76	68.12	
HS2-28		20	28	523.10	66.57		
HS3-28		20	28	550.21	70.02		
HN1-90	0	20	90	400.31	50.94	50.08	
HN2-90		20	90	366.84	46.68		
HN3-90		20	90	413.50	52.62		
HS1-90	1	20	90	598.93	76.22	74.87	49.4
HS2-90		20	90	567.91	72.27		
HS3-90		20	90	598.01	76.10		

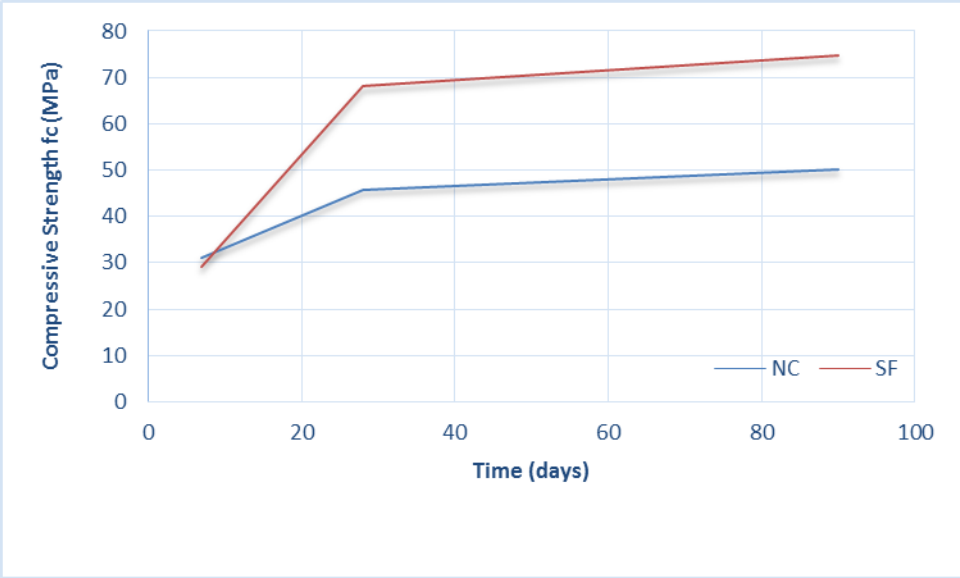

Figure 4.4 Cylindrical compressive strength results with age for normal and SF concrete.

The non-fibrous cylindrical specimens exhibited brittle failure mechanism while the fibrous concrete specimens are quite ductile in the compression test. Hence, SF are very effective in internally confining the concrete. The failure test results are shown in Figure 4.5.

Figure 4.5 Failed cylindrical specimens in compressive test for the present study.

The concluding remarks for studying the effect of SF on the compressive strength are that, the SF has negative effect of the compressive strength at the early each of the concrete mixture this is due to superplasticizer, which has a retardation effect. The compressive strength increased with about 48% for SF mixture compared to the normal concrete. Finally, the failure mode changed from brittle failure for normal concrete cylinders to moderately ductile failure for SF cylinder specimens.

4.2.3 Tensile strength

The tensile strength for plain concrete mixture loosed immediately after formation of the first crack. This is due to well-known fact that, concrete is strong in compression but weak in tension. To overcome this weakness, the addition of SF to concrete mix is added, and to study the improvement in tensile strength of SFRC in indirect tension, 18 cylindrical concrete specimens are casted, cured and tested.

The in direct tensile strength tests are performed on plain concrete (control mix) and on SFRC mixture at the age of 7, 28 and 90 days. Then the tensile strength f_t is calculated based on equation (4.1). Three replicated cylindrical specimens are tested for each test age.

$$f_t = \frac{2P}{\pi D L} \quad (4.1)$$

where, f_t is tensile strength (MPa), P is applied load N, D is diameter of cylindrical specimens (mm), and L is length of cylindrical specimens (mm).

Table 4.3 reports the tensile strength results at 7, 28 and 90 days gained from both plain and SF concrete cylindrical specimens. The results of the splitting tensile strength tests clearly showed the benefit of SF.

The tensile strength has been improved due to addition of hooked ended SF and it will be about 60% greater than that obtained for plain concrete mixture. This is due to the large frictional and SF fiber bending energy developed during fiber pullout on either side of a crack, and due to deformation at multiple cracks when they occur.

Table 4.3 Tensile strength results for plain and SF concrete specimens

Spec. code	***Vf*** *(%)*	***Temp.*** *(°C)*	***age*** *(day)*	***Load*** *(kN)*	***ft*** *(MPa)*	***avg. ft*** *(MPa)*	***Diff.*** %
HN1-7	0	20	7	149.40	4.75	4.94	
HN2-7		20	7	154.42	4.91		
HN3-7		20	7	162.31	5.16		
HS1-7	1	20	7	262.04	8.34	8.07	63.36
HS2-7		20	7	248.15	7.89		
HS3-7		20	7	251.29	7.99		
HN1-28	0	20	28	203.74	6.48	6.63	
HN2-28		20	28	202.72	6.45		
HN3-28		20	28	218.47	6.95		
HS1-28	1	20	28	347.98	11.07	10.84	63.49
HS2-28		20	28	332.39	10.58		
HS3-28		20	28	342.00	10.88		
HN1-90	0	20	90	213.53	6.80	7.01	
HN2-90		20	90	217.50	6.92		
HN3-90		20	90	230.02	7.32		
HS1-90	1	20	90	367.98	11.71	11.48	63.76
HS2-90		20	90	354.01	11.26		
HS3-90		20	90	360.05	11.45		

SF specimens demonstrated higher splitting tensile strength relative to plain specimens at all curing ages as shown in Figures 4.6.This is likely due to increasing the bond between the matrix and fibers which increase the possibility of counteracting crack growth and prevent micro cracks merging to form large cracks. The percent of increase in tensile strength at 7, 28, and 90 curing days is about 63% illustrated in Figure 4.6.

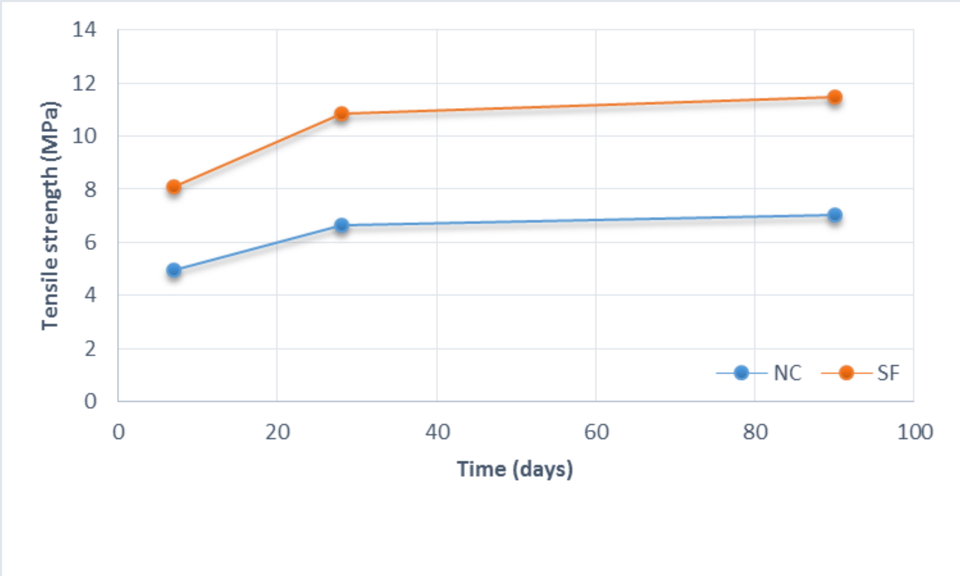

Figure 4.6 Cylindrical tensile strength results with age for normal and SF concrete.

The tested cylinders for plain concrete failed suddenly and split into two separate parts, while the cylinders with SF is cracked at failure without separation, (see Figure 4.7). Thus, the addition of SF change the failure mode form brittle failure for plain concrete to quasi-brittle (ductile) failure mode for SF concrete mixture.

One can conclude that, the SF has significantly improve the tensile strength for concrete mixture and change the failure mode of concrete mix in tension from brittle failure to quasi-brittle or ductile failure.

Figure 4.7 Failed cylindrical specimens in indirect tensile test for the present study.

4.3 Structural Behavior of Steel Fiber Reinforced Concrete

The present experimental program to study the structural behavior of SFRC simply supported beams subjected to a monotonically increased concentrated load, started with, the design of the beam specimens; the beams are designed to fail due to flexure failure prior to the shear failure. A totally of 12 simply supported SFRC beam specimens are constructed and tested.

Prior to listing the analysis results of the present experimental work, a presentation of the structural failure modes of SFRC beams subjected to a monotonically-increased, concentrated load at the mid-span is presented.

A simply supported SFRC beam often fails due to flexural failure, shear failure, or a combination of both. The flexural failure usually happens for beams with little (minimum amount) of flexural (longitudinal) reinforcement, and take place at high moment location. The flexural cracks initiated vertically (perpendicular to the neutral axis) at the tension zone, for the simply supported beams, (see Figure 4.8); the mid third region of the beam is the location where flexure cracks initiated from the bottom layers of the beam and growth upward and wide until the failure of the beam (ductile failure).

While the shear failure happens in beams with an enough to high amount of flexural reinforcement. This failure may occur prior to or after flexural failure. Shear cracks initiated in high shear region (near the support) and it is inclined cracks with an angle of 45° and the spreading toward the center of the beam, (see Figure 4.8), finally, the beam fails with the sudden opening of the critical inclined crack (brittle failure).

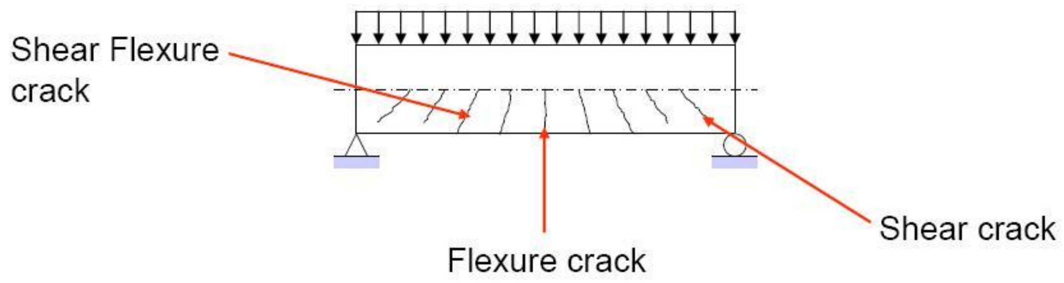

Figure 4.8 Flexural and shear crack for simply supported beams.

The analysis of the behavior of all tested beam specimens are provided in this section. To fully understand the beam behavior, each specimen will be analyzed separately then a comparison between the test results is also be made to investigate the effect of the studied parameters on beam behavior.

A test program matrix is established to study the effect of using different studied parameters on the structural behavior of simply supported SFRC beams with different shear span to depth ratio. The test matrix was divided into five groups based on the objective of each group. The test matrix is shown in Table 4.4.

4.3.1 Group A

This group is consist of two tests on two solid beam specimens. The detailed properties of the tested beams are presented in Chapter 3. A control beam specimen named: N-L8-0-3 with zero SF and without web reinforcement (i.e. stirrups) was tested to compare the results with the same beam specimen with the difference that had SF named: S1-L8-0-3. The beam specimens are slender beams with shear span to depth ration (a/d) equal to 8.Thus, the objective of this group is to study the effect of the SF on reinforced concrete beam without shear reinforcement and discuss the structural behavior of beam specimens.

Table 4.4 Present test program matrix

Group	Beam cross-section	(a/d) ratios	Stirrups	SF ratio	Name
A	solid section	8	φ5.3@1.2 = 3	zero	N-L8-0-3
				1.0%	S1-L8-0-3
	Objective: Study the effect of using SF as an alternative to the stirrups				
B	solid section	8	φ5.3@75 = 32	zero	N-L8-0-32
	Square Hollow type 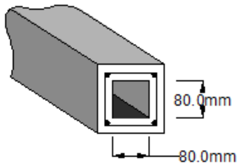	8	φ5.3@75 = 32	zero	N-L8-80-32
	Circular Hollow type 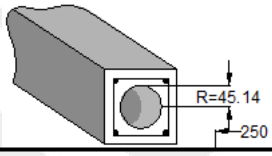	8	φ5.3@75 = 32	zero	N-L8-C80-32
	Objective: Study the effect of hollow cross section types.				
C	solid section	8	φ5.3@75 = 32	1.0%	S1-L8-0-32
	Square Hollow type 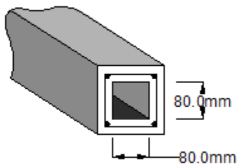	8	φ5.3@75 = 32	1.0%	S1-L8-80-32
	Circular Hollow type 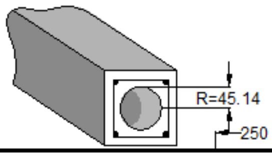	8	φ5.3@75 = 32	1.0%	S1-L8-C80-32
	Objective: Study the effect SF on the hollow cross section types.				
D	Square Hollow type 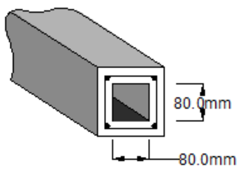	6	φ5.3@75 = 24	1.0%	S1-L6-80-24
		4	φ5.3@75 = 18	1.0%	S1-L4-80-18
	Objective: Study the effect (a/d) on the square hollow type				
E	Circular Hollow type 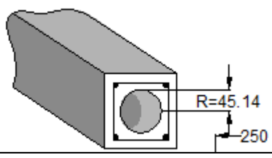	6	φ5.3@75 = 24	1.0%	S1-L6-C80-24
		4	φ5.3@75 = 18	1.0%	S1-L4-C80-18
	Objective: Study the effect (a/d) on the circular hollow type.				

The beam was designed to fail in flexure with tensile mode, which is characterized by the formation of cracks in the tensile stress zone, then yielding of steel bars and shifting the neutral axis toward the compression zone. The general behavior of the tested beam can be described as follows.

At early stages of loading, several flexural cracks first initiated from the bottom surface of the beam in the region under the two loading points, where the maximum constant moment occurred. The first flexural cracks developed at the applied load of approximately 4.4 kN. As the applied load increased, flexural cracks spread out toward the support.

At about 79% of the ultimate load, more flexural cracks developed at the bottom face of the beam, which proceeded towards the main cracks and often joined them. As the load increased, the main central flexural cracks extended upward and become wider, followed by yielding of longitudinal reinforcement. At the ultimate load stage the reinforcement begins to plastic deformation and loss the carrying properties simultaneously with a crushing of concrete under the load that lead to the failure of the beam. The crushing occurred because as the applied load increases the crack at bottom face (tension face) becomes wider at the same time the concrete in the top face was under high compression force, further increase in load caused concrete crushing (i.e., high beam curvature). Crack patterns and the failure shape of the control beam specimen N-L8-0-3 are shown in Figures 4.9 and 4.10 respectively.

The failure of the control beam specimen N-L8-0-), as discussed above, is flexural failure by yielding of the tensile reinforcement followed with a crushing of concrete under the load. Although, the control beam specimen is designed to fail in flexure but also it provided with zero web reinforcement. That is mean; the beam may fail due to shear before flexure failure.

The shear failure happen, when the applied load is sufficient to produce a diagonal tension stress greater than the concrete tensile strength, then an inclined crack occurred, this failure type not take place because the diagonal cracking shear force is carried by the shear resistance of un-cracked high strength concrete in the compression zone.

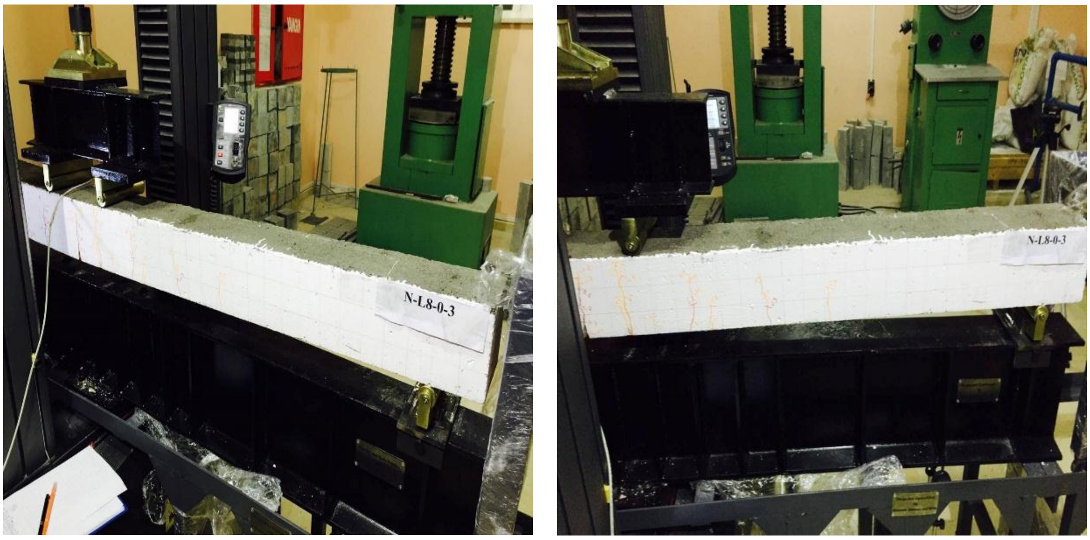

Figure 4.9 Crack pattern for beam specimen N-L8-0-3.

Figure 4.10 Structural failure of beam specimen N-L8-0-3.

The load verses mid-span deflection are recorded, for the control beam specimens (N-L8-0-3), and plotted in Figure 4.11.

The load deflection curve of the control specimen (N-L8-0-3) shows a linear behavior up to about 30% (which is the point of cracking load about 4.4 kN) of the ultimate load this linear behavior due to the fact that, at first loading stages the micro cracks remain undisturbed. For load above cracking point, the deflection curve shows a gradual increase in curvature up to about 80% of the ultimate load , then it bends sharply almost becoming flat at the top reaching the ultimate load about 14.4 kN and finally descends until the specimen is fractured. The mid-span deflection of the beam at cracking point, ultimate point, and fracture point are 2.1, 56.29, and 75.3 mm respectively.

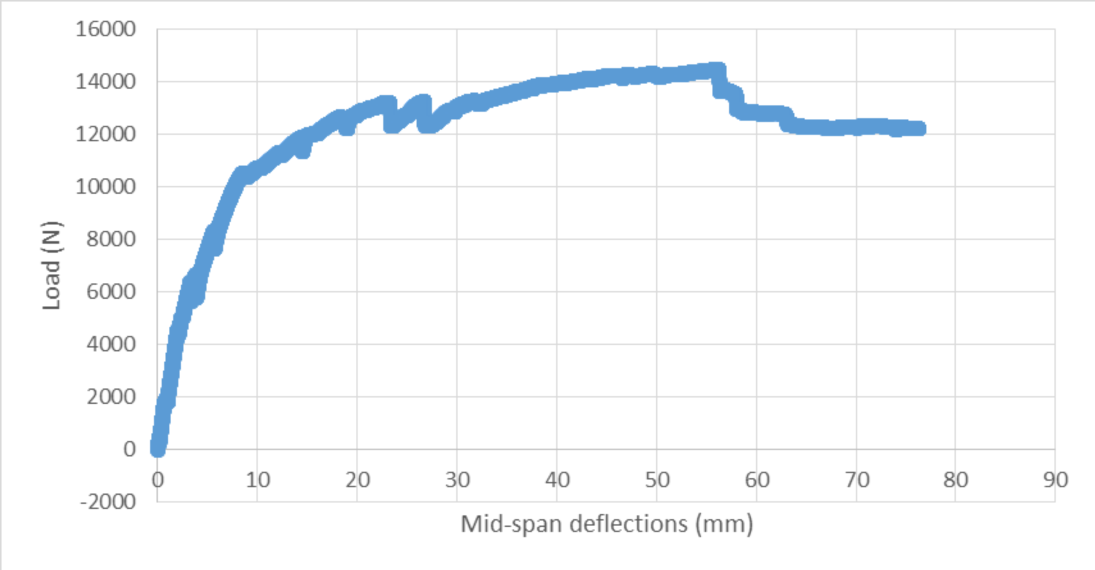

Figure 4.11 Load versus mid-span deflection for the control beam specimen (N-L8-0-3).

The load verses concrete strain at the mid-span are recorded, for the control beam specimens (N-L8-0-3), and plotted in Figure 4.12.

From the results, it can be seen that the strain distribution remains approximately linear at low loads and becomes nonlinear at higher loads due to cracking. At higher load the cracks began widening and more cracks were developed. Then the strain curve bends sharply almost becoming flat at the top (increasing of the strain values with low increment in load) and finally descends until the specimen is fractured. The mid-span concrete strain of the beam at cracking point, ultimate point, and fracture point are 0.00034, 0.00905, and 0.01227 mm/mm respectively.

The hooked ended SF with 1 percent of volume fraction was added to the control beam specimen producing SFRC beam specimen S-L8-0-3. This beam specimen was subjected to monotonically increased two point load with (a/d=8), the objective is to study the effect of the hooked ended SF on the structural behavior of concrete beam without web reinforcement.

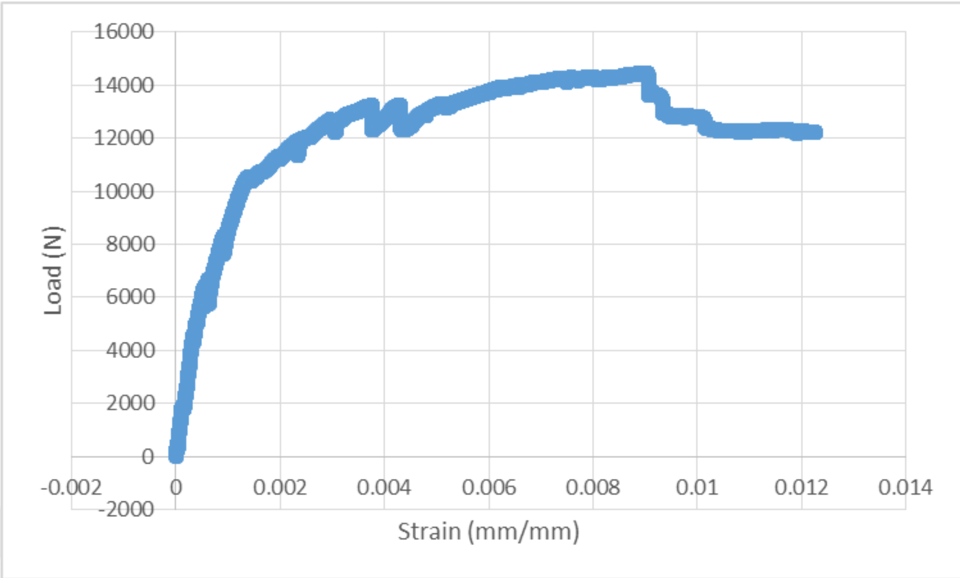

Figure 4.12 Load versus mid-span concrete strain for the control beam specimen (N-L8-0-3).

The behavior of specimen S1-L8-0-3 was started by flexural crack initiated at initial loading stages, these cracks located at the tension face of the beam in the region under the two loading points, where the maximum constant moment occurred. The first flexural cracks developed at the applied load of approximately 16.85 kN which is about four times that that for control specimen N-L8-0-3. Also, as the applied load, increased, flexural cracks do not spread out toward the support as what happened in the control specimen.

Once the specimen S1-L8-0-3 is cracked SFRC composite continues to carry increasing load. As the applied load increased, the main cracks of S1-L8-0-3 beam commenced at the middle zone and the beam exhibited ductile flexural failure. The ductile failure is initiated by yielding of steel reinforcement. The crushing was not visible in beam containing fiber because the fiber changes the mode of failure from brittle to ductile. The presence of the SF also guarantee that, the flexure failure happen and prevent the shear failure, this is due to the fact that, SF substantially increase the shear (diagonal tension) capacity of concrete and mortar beams and can be used effectively in as a minimum shear reinforcement. Crack patterns and the failure shape of the beam specimen S1-L8-0-3 are shown in Figures 4.13 and 4.14 respectively.

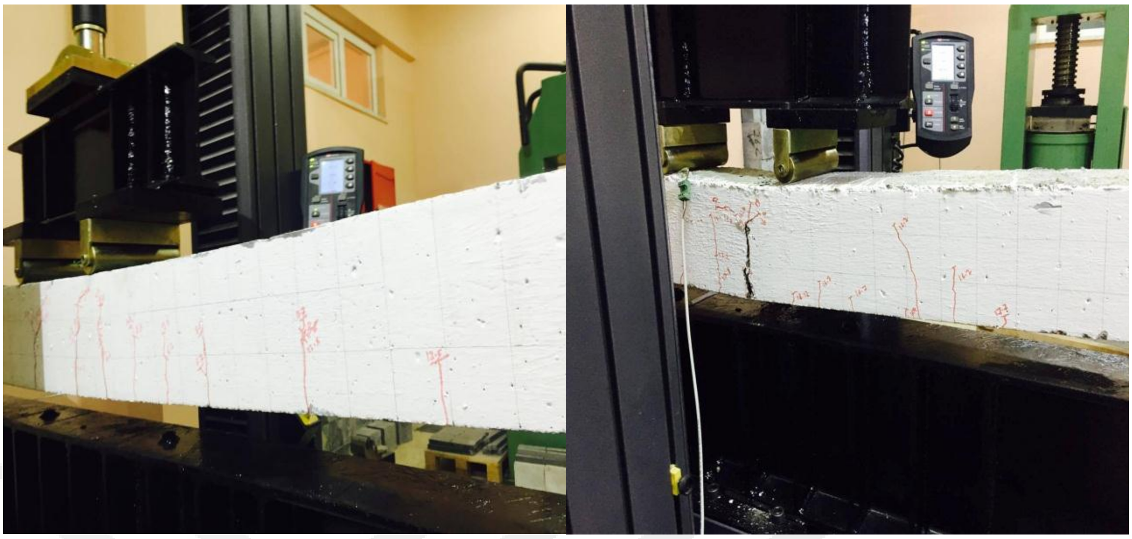

Figure 4.13 Crack pattern for beam specimen S1-L8-0-3.

Figure 4.14 Structural failure of beam specimen S1-L8-0-3.

The peak load of the SFRC composite are greater than those of the concrete matrix alone (specimen N-L8-0-3) during the in elastic range between first cracking load 16.85 kN and the peak load 19.14 kN multiple cracking of SFRC matrix occurs as indicated in Figure 4.15.

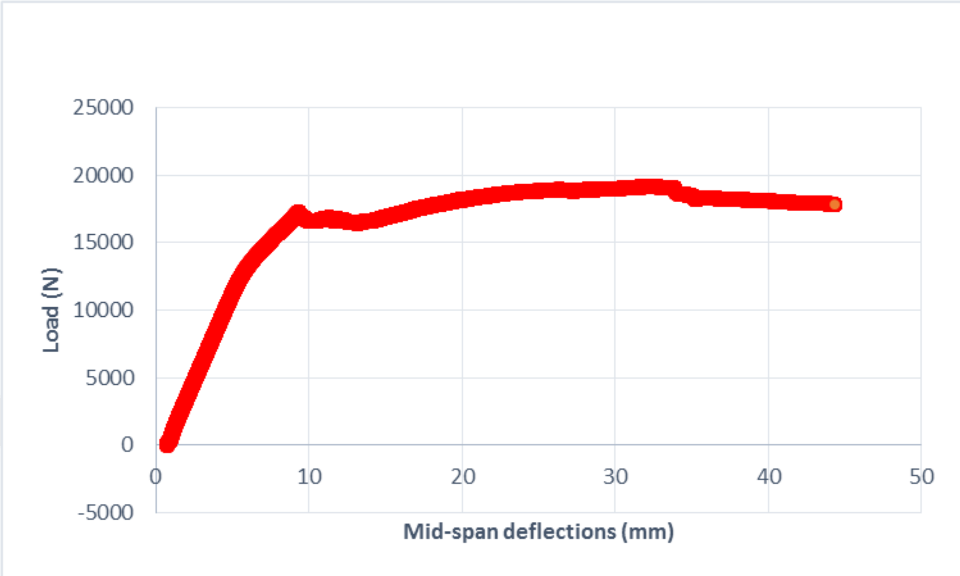

Figure 4.15 Load versus mid-span deflection for the control beam specimen (S-L8-0-3).

The load verses mid-span deflection for both control specimen (N-L8-0-3) and SFRC specimen S1-L8-0-3 are presented in Figure 4.16 from the test results

Figure 4.16 shows the load-deflection curves for slender beams (i.e., specimens N-L8-0-3 and S-L8-0-3) in Group A. It is evident that the addition of hooked ended SF increased the load resistance and energy absorption of the beam specimens. The ultimate load for SF specimen is about 4 times that for the control specimen, while the mid-span deflection for SF specimen at the peak load is about 32.6 mm with a decreasing parentage about 57% in comparison with that of the control specimen 56.29mm.

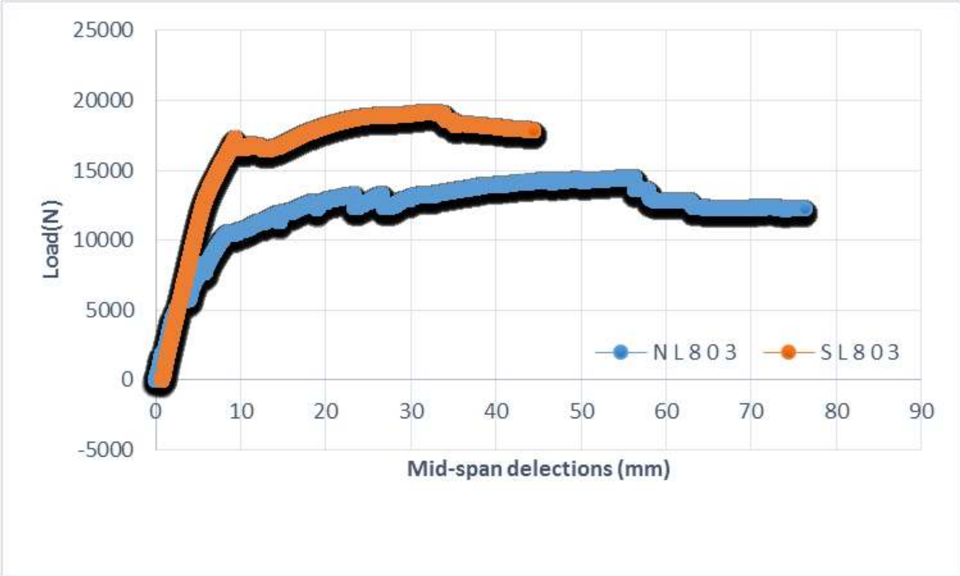

Figure 4.16 Load versus mid-span deflection for both beam specimens (N-L8-0-3) and (S1-L8-0-3).

Figure 4.17 shows the load verse the mid-span concrete strain curves for both specimens N-L8-0-3 and S1-L8-0-3 in Group A. It is apparent that at the elastic range (load level below 4.0 kN) the normal and SF specimens had the same behavior. As the load increased, the behavior of SF specimen is stiffer than the normal specimen. Thus, addition of hooked ended SF decreased the concrete strain at the same load level, that's due to some of applied load is carried by SF. The mid-span concrete strain of the beam at cracking point, ultimate point, and fracture point for beam specimen S1-L8-0-3 are 0.0023, 0.00496, and 0.00702 mm/mm respectively.

The concluding remarks that observed from studying beam specimens of Group A are the high compressive strength concrete for the control specimen (N-L8-0-3) prevent the shear failure (brittle failure) and the specimen failed in yielding of tension reinforcement, and crunching of concrete under the load.

The addition of hooked ended SF improve the structural load resistance approximately about four times, with reduction in structural deflection about 57% in comparison with that of the control specimen. Finally, the shear and crushing failure mode does not take place in SFRC specimen due to SF, which are effective in internally confining the concrete, also prevents and delays the cracks from widening by the contribution of these SF to carry out some of the applied load and work as crack arrestors.

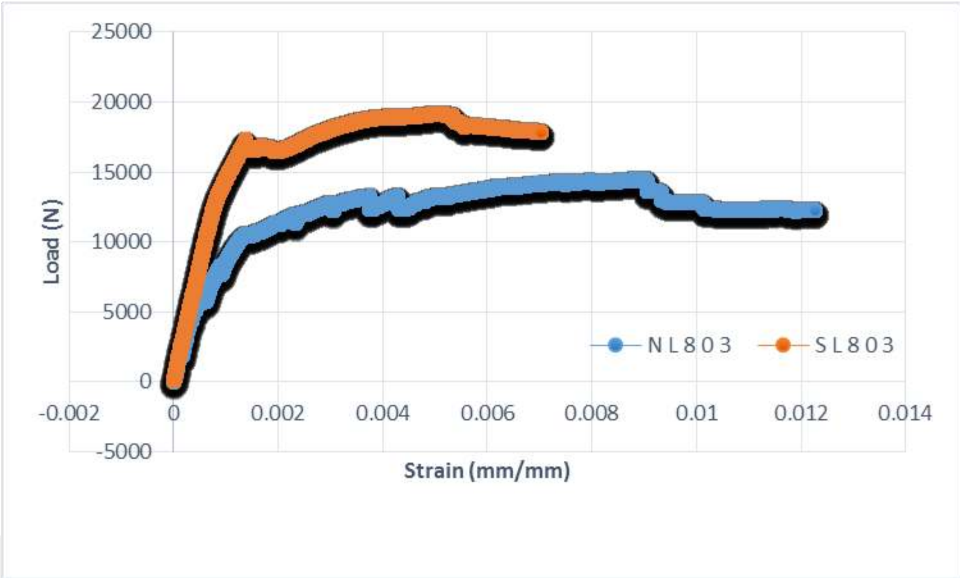

Figure 4.17 Load verses mid-span concrete strains for both beam specimens (N-L8-0-3) and (S1-L8-0-3).

4.3.2 Group B

Three beam specimens (detailed properties for them are provided in Chapter 3) are selected for this group to sever the objective of studying the structural behavior effect of matching the both high strength and lightweight structural member. The control specimen N-L8-0-32 has a solid cross-section while the others specimens N-L8-80-32 and N-L8-C80-32 had square and circular hollow cross-section respectively, (see Figure 4.18 and Table 4.5) with about approximately 30% weight reduction in comparison with the control specimen.

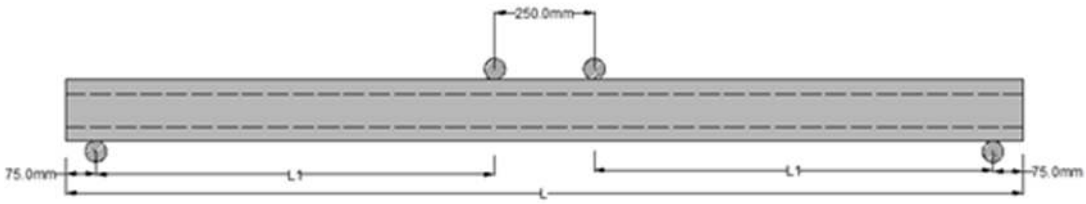

Figure 4.18 Beam specimens span length

Table 4.5 Beam specimen's cross-sectional dimensions.

Specimen Code	*Span length*		*exterior dimensions*		*holes size and numbers*		*weight*	*Weight red.*
	L [mm]	L1 [mm]	H [mm]	B [mm]	h' [mm]	b' [mm]	*(kN/m)*	*(%)*
N-L8-0-32	2450	1000	150	150	0	0	0.55	0
N-L8-80-32	2450	1000	150	150	80	80	0.39	30
N-L8-C80-32	2450	1000	150	150	R = 45.14		0.39	30

The structural behavior of the three beam specimens under two point axially concentrated load as shown in Figure 4.18 exhibit approximately the same behavior that is described by the formation of flexural cracks in the tensile stress zone at the early load stages. The first flexural cracks developed at the applied load of approximately 4.3, 4.25, and 4.3 kN with corresponding mid-span deflection about 2.83, 2.29, and 2.91 mm for specimens N-L8-0-32, N-L8-80-32, and N-L8-C80-32 respectively.

The increase of loading result in spreading out the flexural cracks toward the support moreover, causes the extensions of the main central flexural cracks upward and become wider, followed by yielding of longitudinal reinforcement. At the ultimate load stage, the reinforcement begins to plastic deformation and loss the carrying properties simultaneously with a crushing of concrete, immediately followed by the failure of the beams. Crack patterns and the failure shape of the beam specimens N-L8-0-32, N-L8-80-32, and N-L8-C80-32 are shown in Figures 4.19 and 4.20 respectively.

The load deflection curves for the three beam specimens in Group B are shown in Figure 4.21, one can noted the similarity in the structural behavior for the beam specimens which reflect the benefit of matching the both high strength and lightweight structural member. From this figure, it is noted that the three beams had similar elastic behavior until the load of the first crack that is about 4.0 kN after that the specimens continued in carrying capacity with the new slope in the area of multiple flexural cracking in elastic behavior. The new slope region started from the cracking load until reaching about 75% of the ultimate load.

(a) N-L8-0-32

(b) N-L8-80-32

(c) N-L8-C80-32

Figure 4.19 Crack pattern for beam specimens of Group B.

Figure 4.20 Structural failure for beam specimens of Group B.

As the load increases approximately above the 75% of the ultimate load, the specimens had a drop in deflection curve. (i.e. redaction in slope of load-deflection curve). This reduction in the slope (stiffness) of the specimens came from the development of more flexural cracks leading to increase in the strain of longitudinal reinforcement (yielding of steel reinforcement) until reaching the ultimate load. The final stage, plastic deformation take place in reinforcements simultaneously with a crushing of concrete, immediately followed by the failure of the beams.

The approximate similar load values in the load stages for the three beam specimens with the corresponding mid-span deflections are listed in Table 4.6.

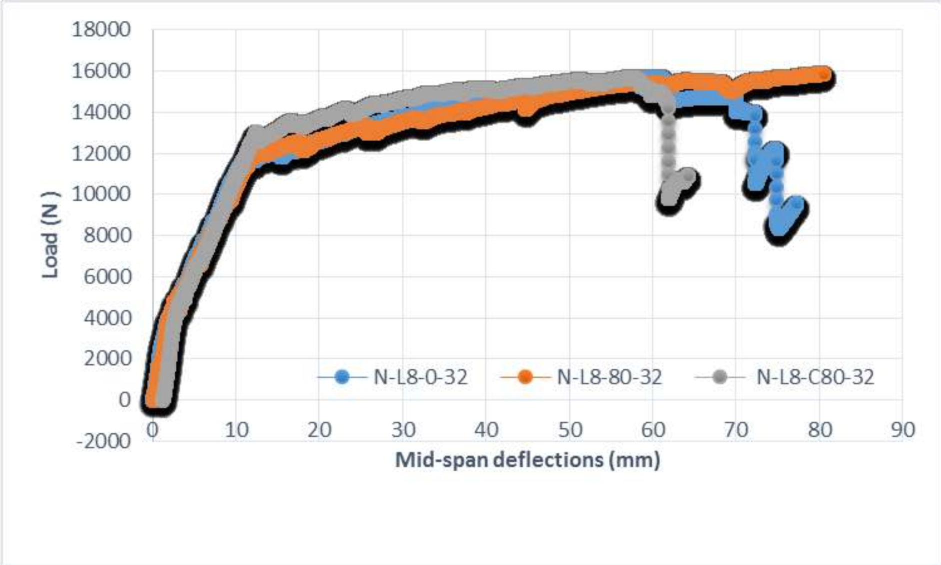

Figure 4.21 load verses mid-span deflections for beam specimens of Group B.

Table 4.6 Beam specimen's load and deflections of Group B.

		Stage I		***zero- cracking load***
Specimen Code	**load** (kN)	**Differences** (±%)	**Deflections** (mm)	**Differences** (±%)
N-L8-0-32	4.3	-	2.38	-
N-L8-80-32	4.2	(-2.32)[1]	2.29	(-3.78)[1]
N-L8-C80-32	4.3	(0.0)[1] (+2.38)[2]	2.91	(+22.26)[1] (+27.07)[2]
		Stage II		***cracking load-75% of ultimate load***
N-L8-0-32	15.6	-	57.59	-
N-L8-80-32	15.4	(-1.2)[1]	58.33	(+1.28)[1]
N-L8-C80-32	15.4	(-1.2)[1] (0.0)[2]	58.01	(+0.72)[1] (≅0.0)[2]
		Stage III		***75% of ultimate load-failure load***
N-L8-0-32	9.5	-	77.24	-
N-L8-80-32	15.8	(+66.31)[1]	80.50	(+4.22)[1]
N-L8-C80-32	10.9	(+14.73)[1] (-31.01)[2]	64.26	(-16.80)[1] (-20.17)[2]

1 difference in comparison to control specimen (N-L8-0-32)
2 difference in comparison to specimen (N-L8-80-32)

The mid-span concrete strain for the specimens in this group exhibit approximately the same behavior at the first load stage (i.e., elastic behavior), and at the multi cracking stage (i.e., from cracking to ultimate loads) also they behave with the same manner as shown in Figure 4.22.

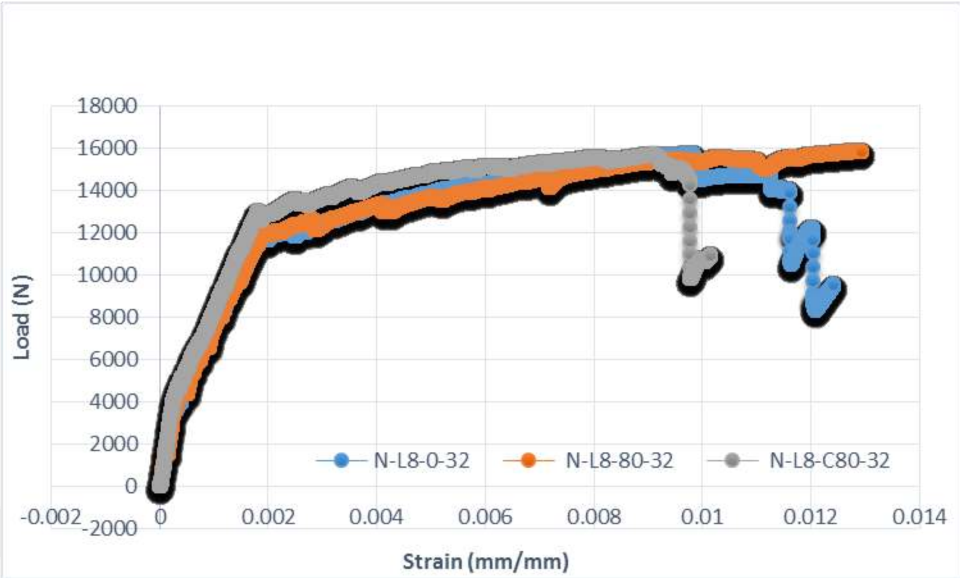

Figure 4.22 load versus mid-span concrete strain for beam specimens of Group B.

The test results presented in Table 4.6 and in Figures 4.21 and 4.22 indicate that, the behavior of the three beam specimens in Group B are approximately with the same manner especially at the first two load stages. Thus, the objective by matching between the lightweight structural members (with a reduction about 30% of the dead load) and high strength concrete gained the aim, and one can recommend the use of high strength hollow cross section concrete beam which is more economical (30% save of members weight) and lead to the same structural behavior of that of the high strength solid concrete section.

4.3.3 Group C

This group is consisted of three beam specimens named: S1-L8-0-32, S1-L8-80-32 and S1-L8-C80-32. These beam specimens are identical to those in Group B (N-L8-0-32, N-L8-80-32 and N-L8-C80-32) with only one difference is the addition of SF with 1% of volume. The objective of this group is to study the effect of SF on the structural behavior on hollow high strength concrete sections in comparison with the control specimen with solid section. As presented in Table 4.5 in Group B the beam weight reduction is about 30% for specimens S1-L8-80-32 and S1-L8-C80-32 compared to the solid specimen S1-L8-0-32.

The specimens tested under two-point load and the results observed. The detected crack patterns for specimens S1-L8-0-32, S1-L8-80-32 and S1-L8-C80-32 are presented in Figure 4.23. These patterns reflect that, the addition of hooked ended steel made the few flexural cracks appears only at the mid third of the span started from the tension face extended upward as load increased with a little distributions of these cracks towards the supports. The main flexural cracks become wider which lead to yield the bottom reinforcement and then the plastic deformation take place in these steel bars followed with immediate failure of the three beam specimens as shown in Figure 4.24.

The load verses mid-span deflections and concrete strain for the three beam specimens in Group C are shown in Figure 4.25 and 4.26 respectively, one can observe that, all beam specimens behave approximately with the same behavior at the elastic range. After the formulation of the first flexural crack the solid section specimen S1-L8-0-32 has stiffer than the others (i.e., withstand the same load with smaller deflection). The first flexural crack appears for the hollow specimens S1-L8-80-32 and S1-L8-C80-32)at loads 6.8 and 7.4 kN respectively, while the stiffer one (S1-L8-0-32) need about 9.6 kN to produce the first crack. At this region, the specimens continued in carrying capacity with the new slope in the area of multiple flexural cracking in elastic behavior as shown in the Figures 4.25 and 4.26.

As the load increases approximately above 15kN, the control solid specimen reach the ultimate load and deflection (15.05 kN, 25.55 mm) and fail in a ductile manner. While beyond this limit 15kN the orientation effect of hooked ended SF appears and change the structural behavior of the hollow specimens. The hollow cross section increase the wall action (i.e., the SF are oriented near the hollow boarders straightly. Thus SF become perpendicularly to the tensile cracks direction) that means the beams had higher load carrying capacity due to tension stiffening, the hollow specimens had increase in slope of load verses deflection and strain curves. The ultimate load for hollow specimens S1-L8-80-32 and S1-L8-C80-32 with the corresponding deflection are (18.5 kN, and 41.85mm) and (17.76 kN, and 41.44

mm). The final stage, plastic deformation take place in reinforcements, immediately followed by the failure of the beams.

(a) S1-L8-0-32

(b) S1-L8-80-32

(c) S1-L8-C80-32

Figure 4.23 Crack pattern for beam specimens of Group C.

(a) S1-L8-0-32

(b) S1-L8-80-32

(c) S1-L8-C80-32

Figure 4.24 Structural failure for beam specimens of Group C.

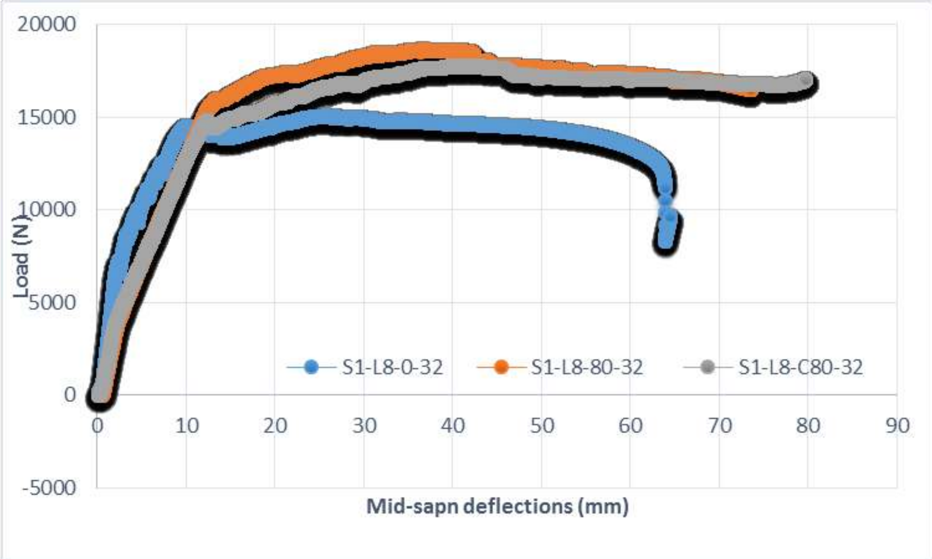

Figure 4.25 Load versus mid-span deflections for beam specimens of Group C.

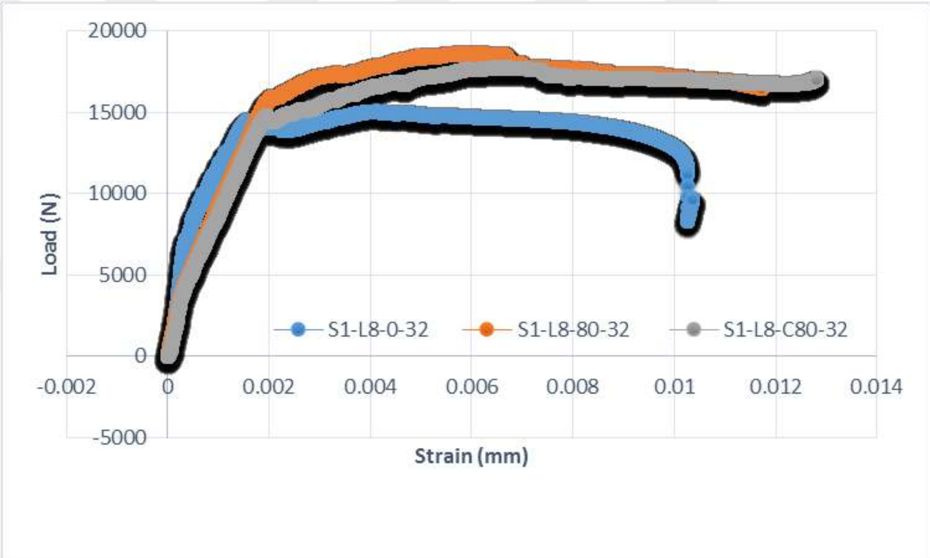

Figure 4.26 Load versus mid-span concrete strain for beam specimens of Group C.

Finally, one can conclude the effect of SF on the behavior of hollow cross section is more effective. That make the choice of matching between the lightweight structural members (with a reduction about 30% of the dead load) and SF high strength concrete is more recommended. To highlight the effect of the addition of the SF on the behavior of high strength hollow specimens. The load verses deflections for hollow normal specimens (N-L8-80-32 and N-L8-C80-32) and hollow SF specimens (S1-L8-80-32 and S1-L8-C80-32) are presented in Figures 4.27 and 4.28 respectively.

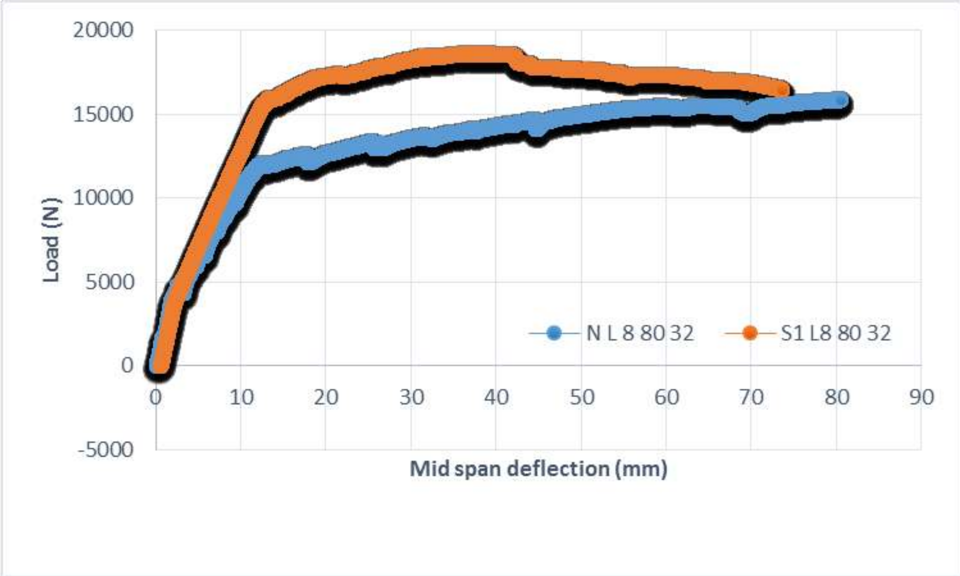

Figure 4.27 Load versus mid-span deflections for beam specimens (N L 8 80 32) and (S1 L8 80 32).

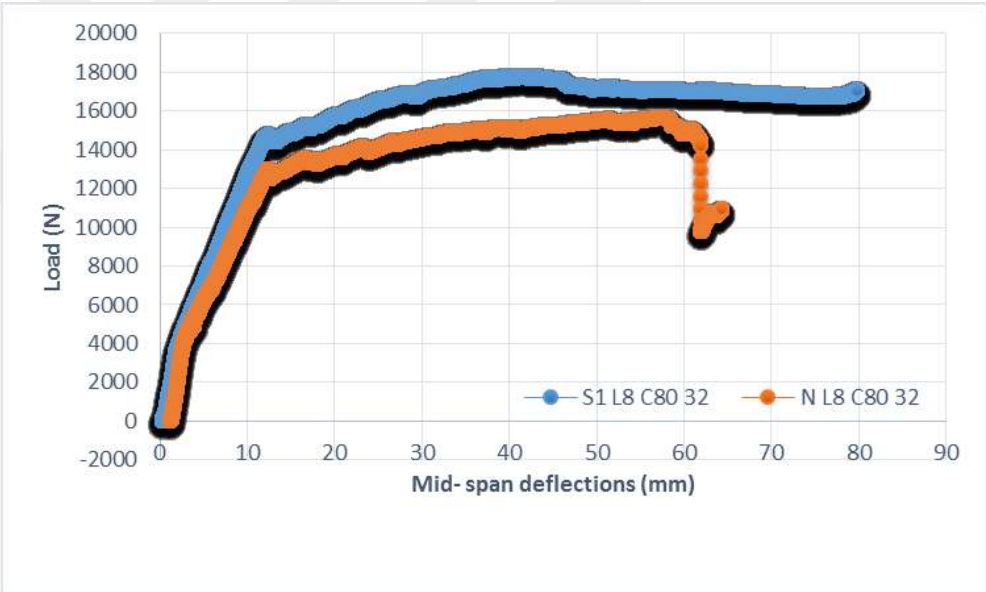

Figure 4.28 Load versus mid-span deflections for beam specimens (N L 8 C80 32) and (S1 L8 C80 32).

The comparison of the results indicate the positive effect of SF in crack-resistant, toughness and the flexural strength improvement of SF beam specimens. The flexural strength improved by about 20% for square hollow type (N-L8-80-32 and S1-L8-80-32), and about 15% for circular hollow type (N-L8-C80-32 and S1-L8-C80-32). Finally, the matching between lightweight structure and SF high strength concrete gave positive results from both structural (increasing in flexural strength about 15%-20%) and economical (30% reduction in dead load) points of views.

4.3.4 Group D

The objective of this group is to study the effect of shear span over the effective depth (a/d) on the structural behavior of hollow square type of SF beam specimens S1-L6-80-24, and S1-L4-80-18, also the specimens details are provided in Chapter 3. Two values of (a/d) are considered in this study, which are 6, and 4.

The high strength hollow concrete section enhanced with SF produce positive structural behavior for slender beam with (a/d= 8) as noted from the results of Group C. The two beam specimens in Group D subjected to two point load, and the crack patterns with the failure shape for the specimen S1-L6-80-24 are shown in Figures 4.29 and 4.30 respectively, while for specimen S1-L4-80-18 are demonstrated in Figures 4.30.

Figure 4.29 Crack pattern for beam specimens S1-L6-80-24.

The visible first crack load of the beam specimen (S1-L6-80-24) appears at load 7.7 kN which is about 37.19% of the experimental ultimate loads, and for specimen S1-L4-80-18 appears at 18.5kN which is about 48.68%. The rest cracks are stared later, and all first cracks were distributed throughout the constant moment region.

Figure 4.30 Structural failure for beam specimens S1-L6-80-24 and S1-L4-80-18.

From above one can note that, the shear span over the depth (a/d) values had affected the appearance of the first crack that is as the (a/d) decreased as the delay in the first flexural crack noted.

The failure mode of the two specimens are flexural failure take place as the applied load increased and take place by yielding of reinforcement in high constant moment region.

The behavior of beam specimens of Group D is shown by the nature of the load verses deflection and strain curves, Figures 4.31 and 4.32 respectively. At low-level loads (stage I), the load mid-span deflection curves are linear representing linear elastic features. Advance increase in loading (stage II) resulted in a few vertical cracks developing within the constant moment region of the beam. At that time the stiffness of the beam reduced by a change in the slope of the load verse deflection curve.

The behavior of these two beam specimens is similar at the first two load stages, but the specimen with short span (S1-L4-80-18) show much stiffness and load carrying capacity than the other specimen S1-L6-80-24. The end limit (load-deflection values) for stage II for specimen S1-L4-80-18 is about (33kN with 8mm), while for specimen S1-L6-80-24 the limit is about (18kN with 20mm). That represent how much the increased in the load carrying capacity for specimen S1-L4-80-18 which is about 83.33% in comparison with specimen S1-L6-80-24 at approximately same deflection value.

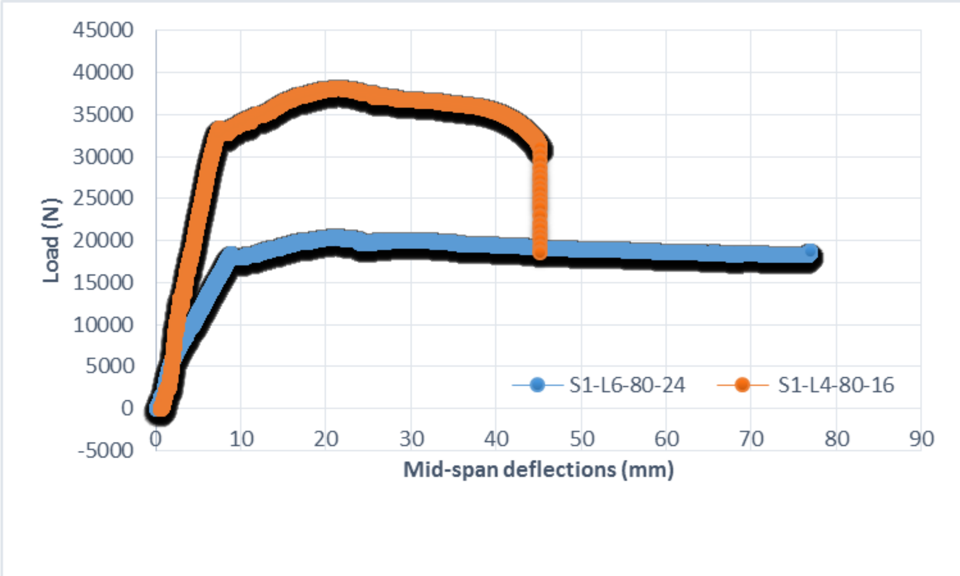

Figure 4.31 Load versus mid-span deflections for beam specimens of Group D.

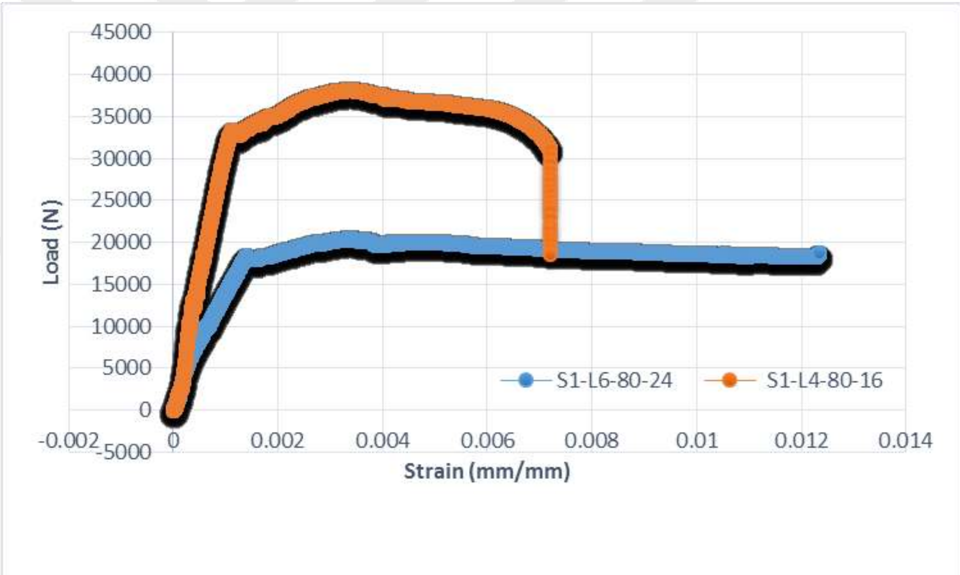

Figure 4.32 Load versus mid-span concrete strain for beam specimens of Group D.

The behavior of the specimens beyond stage II depended on the predicted mode of failure based on their (a/d) values. The beam with (a/d=4) (specimen S1-L4-80-18) is failed by the vertical cracks which developed at the mid-span widened lead to plastic deformation of tension bars resulting in partial ductile behavior. While, the slender beam with (a/d=6) specimen S1-L6-80-24 is failed by yielding of tension bars and crushing of concrete under the load with more ductile behavior. Thus, one can find that, the low value of (a/d=4) provide strong beam with partial ductile behavior in comparison with low load carrying capacity beam with ductile behavior with (a/d=6).

It is worthy of note that the actual realization of load-deflection curve shown in Figure 4.31, reflects the load stages beyond stage II of softening and strength degradation, that is since softening and strength degradation can only be realized in displacement controlled loading systems as done in the present study. The load-deflection curves for the beam specimens of Group D are plotted against the behavior of specimen S1-L8-80-32 with (a/d=8) as shown in Figure 4.33. The objective of these curves is to study and compare the structural behavior of slender beam with (a/d) value equal to 8 to those specimens of Group D. From the figure, it is clear that the load-deflection curve of the slender specimens with (a/d) values 6 and 8 had similar behavior and failure mode; while the short beam as the (a/d) values deceased, they produce stiffer behavior with limited ductile behavior.

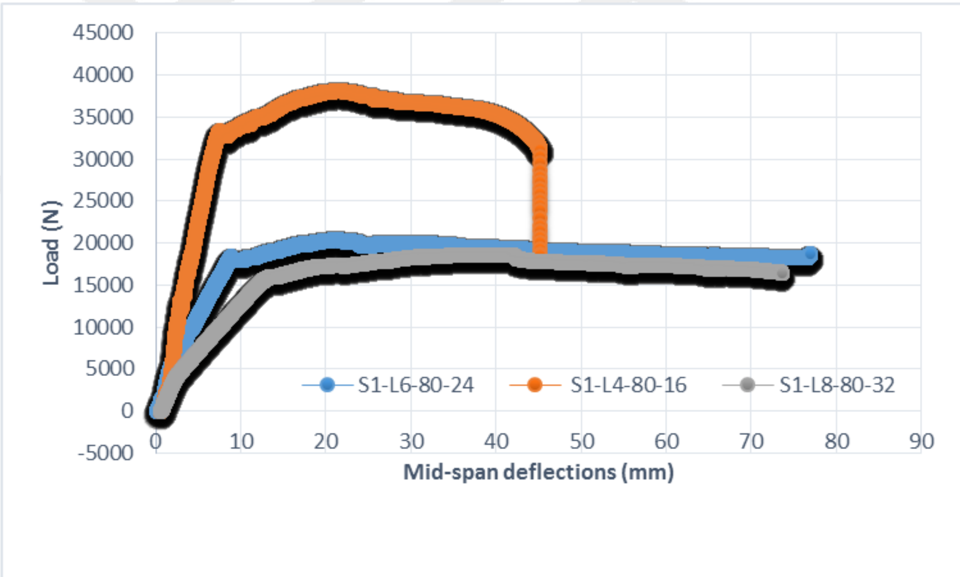

Figure 4.33 Load versus mid-span deflections for beam specimens (S1-L6-80-24), (S1-L4-80-18), and (S1-L8-80-32) .

4.3.5 Group E

The same objective of Group E that, to study the effect of shear span over the effective depth (a/d) on the structural behavior, but in this group the hollow circle type of SF beam specimens (S1-L6-C80-24, and S1-L4-C80-18) are considered. The specimen’s details are provided in Chapter 3. The values of (a/d) considered in this group are 4 and 6.

The crack patterns with the failure shape for the specimens S1-L6-C80-24 and S1-L4-C80-18 are shown in Figures 4.34. For beam specimen S1-L6-C80-24 the first crack appears at about 37.36% of the experimental ultimate loads, cracking load about 6.8 kN and the ultimate load about 18.2kN. While for specimen S1-L4-C80-18 as load reaches 18.5kN, which is about 53% of the ultimate load 34 kN the first crack appears.

(a) (S1-L6-C80-24)

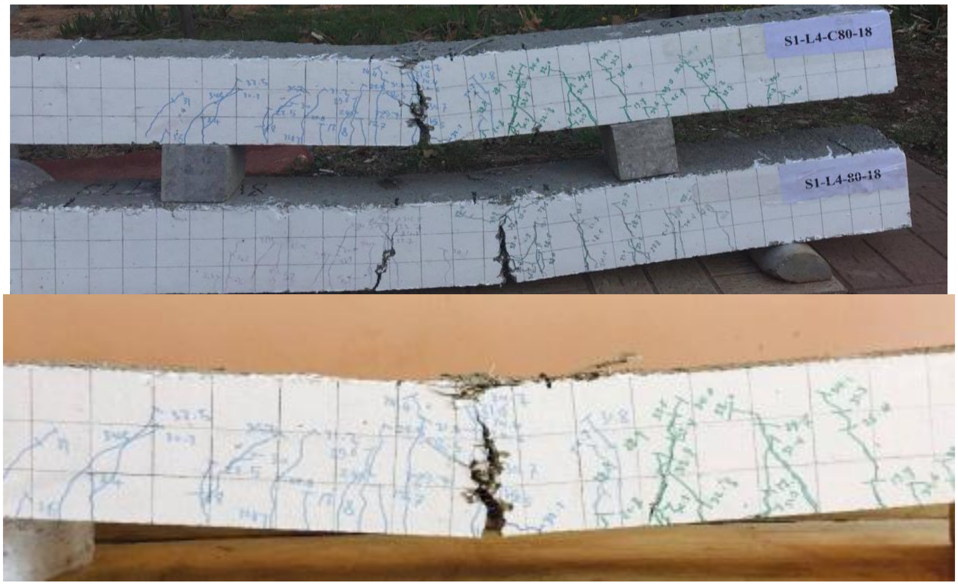

(b) (S1-L4-C80-18)

Figure 4.34 Crack pattern and structural failure for beam specimens of Group E.

The same finding that observed in Group D has taken place for Group E specimens, which is (a/d) values had affected the appearance of the first crack that is as the (a/d) decreased as the delay in the first flexural crack detected.

The structural behavior of beam specimens of Group E is shown by the nature of the load verses deflection curves, (see Figure 4.35). The two specimens behave linearly elastic at the initial load stage with stiffer response for short beam specimen S1-L4-C80-18. As the applied load increased, the central flexural cracks spread out toward the support, and more flexural cracks developed at the bottom face of the beam, which proceeded towards the main cracks and often joined them, as a results the slope load-deflection curves decreased. At advanced load stage, the main central flexural cracks extended upward and become wider, followed by yielding of longitudinal reinforcement, and the inclined shear cracks appears in short specimen S1-L4-C80-18.

At the ultimate load stage, the load-deflection values for specimen S1-L4-C80-18 is about (34kN with 15mm), while for specimen S1-L6-C80-24 the values are (18kN with 25mm). The ultimate load carrying capacity for specimen S1-L4-C80-18 is about 88% greater than that for specimen S1-L6-C80-24. At this stage the reinforcement begins to plastic deformation and loss the carrying properties simultaneously with a crushing of concrete under the load that lead to the failure of the beam. The crushing occurred because as the applied load increases the crack at bottom face (tension face) becomes wider at the same time the concrete in the top face was under high compression force, further increase in load caused concrete crushing (i.e., high beam curvature).

The same concluding remark for Group D is observed that is, the low value of (a/d=4) produce strong beam with partial ductile behavior in comparison with ductile low load carrying capacity with (a/d=6).

The comparison of the structural behavior of SF hollow concrete section with circular hollow type are made for three values of (a/d) which is 4,6, and 8. This is through plotted the load-deflection curves for beam specimens S1-L6-C80-24, S1-L4-C80-18, and S1-L8-C80-32 as shown in Figure 4.36. From the results, it is clear that the load-deflection curve of the slender specimens with (a/d) values 6 and 8 had similar behavior and failure mode; while the short beam as the (a/d) values decreased, they produce stiffer behavior with limited ductile behavior (i.e., the same behavior of specimens with hollow square type).

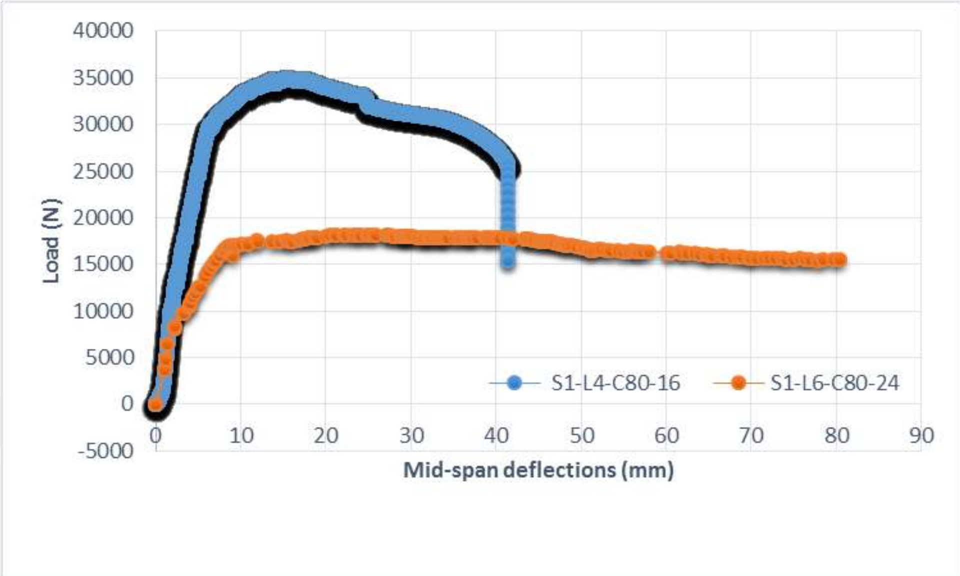

Figure 4.35 Load versus mid-span deflections for beam specimens of Group E.

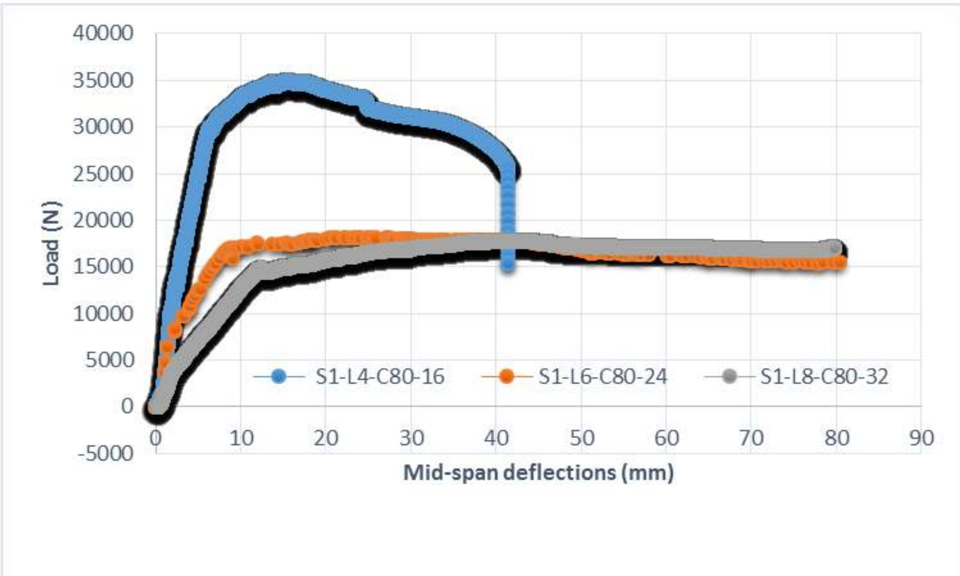

Figure 4.36 Load versus mid-span deflections for beam specimens S1-L6-C80-24, S1-L4-C80-18, and S1-L8-C80-32.

Finally, one can conclude that, the matching between high strength SFRC and lightweight section gave good structural behavior and load carrying capacity as compared with the solid section. Thus, the use of high strength SFRC hollow sections are recommended to produce slender section with long span beams, and at the end these beams section pass the structural and economical points of view in a successful manner. The hollow circular type section although it behave approximately like that of hollow square type, but the recommendations goes to the hollow circular section to overcome the weak point developed at the corner of hollow square section due to stress concentration at these locations.

CHAPTER 5

CONCLUSIONS AND RECOMMENDATIONS

4.4 Introduction

The objective of this chapter is to cover the conclusion remarks that had been observed from the investigation of effect of adding hooked ended SF for high strength reinforced concrete members. This experimental work is attempt to matching the both lightweight structural member with the structural ductility requirements. This reached by combining the optimum beam's section topology with using SF reinforcement. Different parameters are used to alter, named, shear span to depth ratio (a/d) and hollow shape. Three values for (a/d) used for investigating 8, 6, and 4. Two hollow type of circular and square shape are used.

The conclusions derived from this study along with recommendations for future work-studies related to the topic of this work are provided.

4.5 Conclusions

The following conclusions are drawn from present study:

1. The addition of hooked ended SF to concrete reduces the flow characteristics and workability of the concrete mixture.
2. The existence of hooked ended SF in a concrete mixture advance the toughness of SFRC in compression, that's means increase of the ability to absorb energy during deformation, which change the failure mode from brittle failure for normal concrete cylinders to moderately ductile failure for SF cylinder specimens.
3. The SF has negative effect of the compressive strength at the early ages (7days) of the concrete mixture this is due to super plasticizer, which has a retardation effect.

4. Based on the results of present compressive test work, the compressive strength increased with about 48% for SF mixture compared to the normal concrete for up to 1.0 percent by volume of SF.
5. The primary benefits of adding SF to concrete is improve the tensile response which results in the incensement of the tensile strength of concrete ranging from 58 -62% for up to 1.0 percent by volume of fibers. Also, change the failure mode of concrete mix in tension from brittle failure to quasi-brittle or ductile failure.
6. The actual realization of load-deflection curves for beam specimens presented in this study, reflects the advanced load stages of softening and strength degradation, that is since softening and strength degradation can only be realized in displacement controlled loading systems as done in the present study.
7. For beams of Group A:
    - The high strength concrete prevent happen of the shear failure because the diagonal cracking shear force is carried by the shear resistance of un-cracked high strength concrete in the compression zone and the specimen failed in yielding of tension reinforcement, and crunching of concrete under the load..
    - The addition of hooked ended SF increased the load resistance and energy absorption of the beam specimen. The ultimate load for SF specimen is about 4 times that for the control specimen, while the mid-span deflection for SF specimen at the peak load is decreased about 57% in comparison with that of the control specimen.
    - Finally, the shear and crushing failure mode does not take place in SFRC specimen due to SF, which are effective in internally confining the concrete, also prevents and delays the cracks from widening by the contribution of these SF to carry out some of the applied load and work as crack arrestors.
8. For beams of Group B:
    - The behavior of the three beam specimens are approximately with the same manner especially at the first two load stages.
    - The objective by matching between the lightweight structural members and high strength concrete gained the aim, and the use of high strength hollow cross section

concrete beam which is more economical (30% save of members weight) and lead to the same structural behavior of that of the high strength solid concrete section.

9. For beams of Group C:
   - The presence of SF has positive effect in crack-resistant, toughness and the flexural strength improvement of SF beam specimens. The flexural strength improved by about 20% for square hollow type and about 15% for circular hollow type.
   - The matching between lightweight structure and SF high strength concrete gave positive results from both structural (increasing in flexural strength about 15%-20%) and economical (30% reduction in dead load) points of views.
10. For beams of Group D:
   - The appearance of the first crack has affected by the shear span over the depth (a/d) values, as the (a/d) decreased as the delay in the first flexural crack noted was observed.
   - The load-deflection curve of the slender specimens with (a/d) values 6 and 8 had similar behavior and failure mode; while the short beam as the (a/d) values deceased equal 4, they produce stiffer behavior with limited ductile behavior.
11. For beams of Group E:
   - The hollow types (i.e., square and circular) beam specimens had the same structural behavior, which is (a/d) values had affected the appearance of the first crack that is as the (a/d) decreased as the delay in the first flexural crack detected.
   - The low value of (a/d=4) produce strong beam with partial ductile behavior in comparison with ductile low load carrying capacity with (a/d=6, and 8).
12. The matching between high strength SFRC and lightweight section gave good structural behavior and load carrying capacity as compared with the solid section.
13. The hollow circular type section although it behave approximately like that of hollow square type, but the recommendations goes to the hollow circular section to overcome the weak point developed at the corner of hollow square section due to stress concentration at these locations.

4.6 Recommendations

After completion of this investigation, it is recommended that future work should investigate the effects of:

1. Different volume fractions of SF on concrete properties and structural behavior.
2. Effects of different lengths of SF on mechanical properties of hardened concrete.
3. Effect of hybrid fiber (combination of steel and polypropylene fiber) on mechanical properties and structural behavior of high strength concrete.
4. SF on structural behavior for deep beams (i.e., shear span over the depth a/d less than 2.0).
5. Investigate the behavior of SF concrete beams with T and I sections and study the result of SF spreading in the web region.
6. Make a finite element model based on the results of the present experimental study.

REFERENCES

[1] Nilson, A. H., Darwin, D., Dolan, C.W. (2004). Design of concrete structures. 13th edition. USA: The McGraw-Hill Companies.

[2] Mcormac, J. C., Brown, R. H. (2015). Design of reinforced concrete. John Wiley & Sons.

[3] ACI. American Concrete Institute . Committee 544, (2008). State-of-the-art report on fiber reinforced concrete ACI 544.1R96 (reapproved 2002). ACI Manual of Concrete Practice, Part 6, pp. ACI544.1R-7ACI544.1R-24

[4] ACI-ASCE. American Concrete Institute. Committee 426 (1973). The shear strength of reinforced concrete Members, *ACI journal Proceedings,* **70(7)**, 471-473.

[5] American Concrete Institute (ACI) Committee 318. (2014). Building Code Requirements for Structural Concrete (ACI 318M-14) and Commentary.Farmington Hills, MI: ACI

[6] ACI SP 142-94 (1991) Fiber Reinforced Concrete—Developments and Inno Boston and Dallas vations, edited by J. I. Daniel and S. P. Shah, Proceedings, Symposia, Boston and Dallas.

[7] Rai, A., Joshi, Y. P. (2014). Applications and properties of fiber reinforced concrete, *Journal of Engineering Research and Applications*, **4**, 123-131.

[8] ASTM. American Society for Testing and Materials. C 1116. (1998) Specification for fiber reinforced concrete and shotcrete. American Society for Testing and Materials, Philadelphia, PA

[9] ACI. American Concrete Institute. Committee 544.4R-88 (1999). Design considerations for steel fiber reinforced concrete , American Concrete Institute, Farmington Hills.

[10] ACI. American Concrete Institute. Committee ACI116R-00 (2000). Cement and Concrete Terminology, American Concrete Institute, Farmington Hills.

[11] Naaman, A. E. (2008). High performance fiber reinforced cement composites. *Naaman A.E. High-performance construction materials: science and applications. Singapore: World Scientific Publishing*, 91-153

[12] Swamy, R. N. (2000). FRC for sustainable infrastructure regeneration and rehabilitation. In P. Rossi, & G. Chanvillard (Eds.), *Fifth International RILEM Symposium on Fibre-Reinforced Concrete (FRC),*3-18.RILEM Publications SARL.

[13] Naaman, A. E. (2000). Fiber reinforcement for concrete: Looking back, looking ahead. In *Proceedings of Fifth RILEM Symposium on Fiber Reinforced Concretes (FRC)* 65-86. RILEM Publications,(2000) SARL.

[14] Johnston, C. D.(2010). *Fiber-reinforced cements and concretes* , **3** , Crc Press.

[15] Choi, J. I., Lee, B. Y. (2015). Bonding properties of basalt fiber and strength reduction according to fiber orientation. *Materials*, **8(10)**, 6719-6727.

[16] Swamy, R. N. (1975). Fibre reinforcement of cement and concrete. *Matériaux et Construction*, **8(3),** 235-254.

[17] Bentur, A., Mindess, S. (2006). *Fibre reinforced cementitious composites*. CRC Press.

[18] Majumdar, A. J. (1975). Fibre cement and concrete—a review. *Composites*, **6(1),** 7-16.

[19] Panzera, T. H., L. Christoforo, L. F., and Ribeiro,P.H., (2013), High performance fiber reinforced concrete (FRC) for civil engineering applications, Woodhead Publishing Limited.

[20] Roumaldi, J. P., Batson, G. B. (2008). *Mechanics of crack arrest in concrete*.

[21] Shah, S. P., Daniel, J. I., Ahmad, S. H., Arockiasamy, M., Balaguru, P. N., Ball, C. G., Casamatta, D. (1993). Guide for specifying, proportioning, mixing, placing, and finishing steel fiber reinforced concrete. *ACI Materials Journal*, *90*(1), 94-101.

[22] ACI. American Concrete Institute. Committee 544 Measurement of Properties of Fiber Reinforced Concrete (ACI-544, 2R), American Concrete Institute, Detroit, 1999.

[23] ACI. American Concrete Institute. 544.5R-10, Report on the Physical properties and Durability of Fiber-Reinforced Concrete. American Concrete Institute,Farmington Hills,MI, 2010.

[24] Batson, G. (1976). Steel fiber reinforced concrete. *Materials Science and Engineering*, **25**, 53-58.

[25] Kang, T. H., Kim, W., Kwak, Y. K., & Hong, S. G. (2011). Shear testing of steel fiber-reinforced lightweight concrete beams without web reinforcement. *ACI Structural Journal*, ***108*(5),** 553.

[26] Karihaloo, B.L., and Wang, J, (2000), Micromechanics of Fiber Reinforced Cementitious Composites, in Materials for Buildings and Structures. Edited by F. H. Wittmann Wiley-VCH Verlag GmbH, Weinheim. 93-111.

[27] Gupta, R.(1999). Hybrid reinforced concrete members: fiber synergy in very high strength concrete. MSc thesis, Pune University.

[28] Lequesne, R.D. (2011). Behavior and Design of High-Performance Fiber-Reinforced Concrete Coupling Beams and Coupled-Wall Systems, PhD thesis, University of Michigan.

[29] Banthia, N. (2010). SP-268: Fiber Reinforced Concrete in Practice. *Special Publication*, 268.

[30] ACI. American Concrete Institute. Committee 116 (2000). Cement and Concrete Terminology, ACI 116R-00, American Concrete Institute, Farmington Hills.

[31] Vairagade, V. S., and Kene, K.S.(2012). Introduction to Steel Fiber Reinforced Concrete on Engineering Performance of Concrete. *International Journal of Scientific & Technology Research*, **1**, 133-142.

[32] ACI. American Concrete Institute. Committee 544 (1996). Design Considerations for Steel Fiber Reinforced Concrete, ACI 544.4R-88, American Concrete Institute, Farmington Hills.

[33] ASTM. American Society for Testing and Materials. A 820/A 820M – 06. (2006) Standard Specification for Steel Fibers for Fiber-Reinforced Concrete, American Society for Testing and Materials, Philadelphia, PA.

[34] Naaman, A. E., and Najm, H., (1991), Bond-slip Mechanisms of Steel Fibers in Concrete, *ACI Materials Journal*, **88(2)**, 135-145.

[35] Trottier, J.F. and Banthia, N., (1994). Toughness Characteristic of Steel-Fibers in Concrete, *ACI Materials Journal*, **88(2)**, 135-145.

[36] Soroushian, P. and Bayasi, Z., (1991) Fiber Type effects on the Performance of Steel Fiber Reinforced Concrete, *ACI Materials Journal*, **88,** No.2, 129-134.

[37] Wu, Z., Shi, C., and He, W., (2016). Effects of steel fiber content and shape on mechanical properties of ultra-high performance concrete, *Journal of Construction and Building Materials*,**103**, 8-14

[38] Yazıcı, Ş., İnan, G., Tabak, V. (2007). Effect of aspect ratio and volume fraction of steel fiber on the mechanical properties of SFRC, *Construction and Building Materials*, **21(6),** 1250-1253.

[39] Deluce, J. R., and Vecchio, F. J. (2013). Cracking Behaviour of Steel Fiber Reinforced Concrete Containing Conventional Steel Reinforcement, *ACI Structural Journal,* **110**, No. 3, 481-490.

[40] Rossi, P., Acker, P., and Malier, Y. (1987). Effect of Steel Fibers at Two Different Stages: The Material and Structure, *Materials and Structures*, **20**, 436-439.

[41] Zollo, R.F., (1979). Fiber-reinforced Concrete: an Overview after 30 Years of Development, *Cement and Concrete Composite*, **19,** 107-122.

[42] Jain, K., and Singh, B. (2013). Steel fibers as minimum shear reinforcement in reinforced concrete beams, Magazine of Concrete Research, **65**, 430– 440.

[43] Banthia, N., and Trottier, J. F.(1995). Concrete Reinforced with Deformed Steel Fibers, Part II: Toughness Characterization, *ACI Material Journal*, **92**, No 1-6, 146-154.

[44] Torrents, J. M., Blanco, A., Pujadas, P., Aguado, A., Juan-Garcı, P. (2012). Inductive method for assessing the amount and orientation of steel fibers in Concrete, *Materials and Structures* , **45**, 1577–159.

[45] Rostbsy, F.S. and Hartwich, K. (1985). Compressive strength and deformation of steel fiber reinforced concrete under high rate of strain, *The international Journal of Cement Composites and Lightweight Concrete*, **7,** 21-28.

[46] Taerwe, L., & Van Gysel, A. (1996). Effect of steel fibers on the design stress—Strain curve for high strength concrete subjected to axial compression. *Mechanics of composite materials*, ***32*(2),** 122-129.

[47] Campione, G., & Mindess, S. (2005). Size effect in compression of high strength fibre reinforced concrete cylinders subjected to concentric and eccentric loads. *Materials for Buildings and Structures, **6**,* 86-91.

[48] Oliveira Júnior, L. Á. D., Borges, V. E. D. S., Danin, A. R., Machado, D. V. R., Araújo, D. D. L., Debs, E. & Rodrigues, P. F. (2010). Stress-strain curves for steel fiber-reinforced concrete in compression. *Matéria (Rio de Janeiro)*, **15(2),** 260-266.

[49] Bencardino, F., Rizzuti, L., Spadea, G., Swamy, R.N., (2008) Stress–strain behavior of steel fiber-reinforced concrete in compression, *Journal Mater Civil Eng*., **20**, 255–263

[50] Hsu, L. S., Hsu, C. T. (1994). Stress-strain behavior of steel-fiber high-strength concrete under compression, *Structural Journal*, **91(4),** 448-457.

[51] Nataraja, M. C., Dhang, N., Gupta, A. P., (1999). Stress-strain curves for steel-fiber reinforced concrete under compression, Cement & Concrete Composites, **21**, 383-390

[52] Lee, S. C., Oh, J. H., and Cho, J. Y. (2015). Compressive Behavior of Fiber- Reinforced Concrete with End-Hooked Steel Fibers Materials, **8,** 1442-1458.

[53] Hughes, B. P., & Fattuhi, N. I. (1977). Stress-strain curves for fiber reinforced concrete in compression, *Cement and Concrete research*, **7(2),** 173-183.

[54] Fanella, D. A., and Naaman, A. E. (1985). Stress-Strain Properties of Fiber Reinforced Concrete in Compression, *ACI Journal*, **82**, No. 4, 475-483.

[55] Otter, D. E., and Naaman, A. E. (1988). Properties of Steel Fiber Reinforced Concrete Under Cyclic Loading, *ACI Materials Journal*, **85**, No.4, 254-261.

[56] Singh, S. P., Singh, A. P., & Bajaj, V. (2010). Strength and flexural toughness of concrete reinforced with steel–polypropylene hybrid fibers, *Asian journal of civil engineering (building and housing)*, **11(4),** 494-507.

[57] Fischer, G., & Li, V. C. (2007). Effect of fiber reinforcement on the response of structural members, *Engineering Fracture Mechanics*, **74(1),** 258-272.

[58] Casanova, P., Rossi, P., and Schaller, I. (1997). Can Steel Fibers Replace Transverse Reinforcements in Reinforced Concrete Beams, *ACI Materials Journal*, **94**, No.5, 341-355.

[59] Meng, Y., Chengkui, Y., and Jizhong, W. (2006). Characteristics of Stress-strain Curve of High Strength Steel Fiber Reinforced Concrete under Uniaxial Tension, *Journal of Wuhan University of Technology - Mater. Sci. Ed.*, **21,** 132-137.

[60] Mangat, P. S. (1976). Tensile strength of steel fiber reinforced concrete, *Cement and Concrete Research*, **6(2),** 245-252.

[61] Gopalaratnam, V. S., Shah, S. P. (1987). Tensile failure of steel fiber-reinforced mortar. *Journal of Engineering Mechanics*, **113(5),** 635-652.

[62] Naaman, A. E., Shar, S. R. (1976). Pull-out mechanism in steel fibre-reinforced concrete. *Journal of the Structural Division*, 102.

[63] Swamy, F. N., Sa'ad, A. (1981). Deformation and Ultimate Strength in Flexure of Reinforced Concrete Beams Made with Steel Fiber Concrete, *American Concrete Institute Journal*, **78** No. 5, 395 - 405.

[64] Shaaban, A. M. and Gesund, H. (1993). Splitting Tensile Strength of Steel Fiber Reinforced Concrete Cylinders Consolidated by Rodding or Vibrating, *ACI Materials Journal*, **90**, No.4, 366-369.

[65] Yao, W., Li, J., and W, K. (2003). Mechanical Properties of Hybrid Fiber-Reinforced Concrete at Low Fiber Volume Fraction, *Cement and Concrete Research*, **33**, 27-30.

[66] ASTM. American Society for Testing and Materials. C 78 (2004). Standard Test Method for Flexural Strength of Concrete (Using Simple Beam with Third-Point Loading), Annual Book of ASTM Standards.

[67] ASTM. American Society for Testing and Materials. C1018 (1997). ASTM Standard C1018 Standard Test Methods for Flexural Toughness and First-crack Strength of Fiber-reinforced Concrete (using beam with third-point loading), ASTM International, West Conshohocken, PA.

[68] ASTM. American Society for Testing and Materials. C1609/C1609M (2008). ASTM C1609/C1609M Standard Test Methods for Flexural Performance of Fiber-reinforced Concrete (using beam with third-point loading). ASTM International, West Conshohocken, PA.

[69] Swamy, R. N., Mangat, P. S. (1974). A theory for the flexural strength of steel fiber reinforced concrete. *Cement and Concrete Research*, **4(2),** 313-325.

[70] Swamy, R. N. (1975). Fiber Reinforcement of Cement and Concrete, *Journal of Materials and Structures*, **8**, No.45, pp235-254.

[71] ACI. American Concrete Institute. SP-155 (1995). Testing of Fiber reinforced concrete, editors: Stevens, Banthia, N., Gopalaratnam, V. and. Tatnall, P. C., American Concrete Institute, Detroit, Michigan.

[72] Banthia, N., Trottier, J. F. (1995). Test Methods for Flexural Toughness Characterization of Fiber Reinforced Concrete: Some Concerns and a Proposition, *ACI Materials Journal*, **92**, 48-57.

[73] Lok, T. S., Xiao, J. R. (1999). Flexural strength assessment of steel fiber reinforced concrete. *Journal of Materials in Civil engineering*, **11(3),** 188-196.

[74] Abdul-Ahad, R. B., Aziz, O. Q. (1999). Flexural strength of reinforced concrete T-beams with steel fibers, *Cement and Concrete Composites*, **21(4),** 263-268.

[75] Yang, I. H., Joh, C., Kim, B. S. (2011). Flexural strength of ultra high strength concrete beams reinforced with steel fibers. *Procedia engineering*, **14,** 793-796.

[76] Padmarajaiah, S. K., and Ramaswamy, A. (2004). Flexural strength predictions of steel fiber reinforced high-strength concrete in fully/partially prestressed beam specimens, Cement & Concrete Composites, **26,** 275–290.

[77] Fu, C. Q., Jin, X. Y., Jin, N. G. (2009). Numerical Experiment on Flexural Properties of Steel Fiber Reinforced Concrete Beam. In *Computer Science and Information Engineering, WRI World Congress on* **7,** 755-759

[78] EI-Niema, E. I. (1999). Reinforced Concrete Beams with Steel Fibers under Shear, *ACI Structural Journal*, **88**, No.2, 178-183.

[79] Swaddiwudhipong, S., Shanmugam, N. E. (1985). Fiber-Reinforced Concrete Deep Beams with Openings, *Journal of Structural Engineering*, **111(8),** 1679-1690.

[80] Tan, K. H., Murugappan, K. and Paramasivam, P. (1993). Shear Behavior of Steel Fiber Reinforced Concrete Beams, *ACI Structural Journal* , **89,** No.6, 3-11.

[81] Majdzadeh, F., Soleimani, S. M., and Banthia, N. (2006). Shear strength of reinforced concrete beams with a fiber concrete matrix, *Canadian Journal in Civil Engineering,* **33,** 726-734.

[82] Sahoo, D. R. and Chao, S. H. (2010). Use of Steel Fiber Reinforced *R* Large Openings, Structures Congress. Editors: Senapathi, S, Casey, K., and Hoit, M., Orlando, Florida, USA , 1981-1991.

[83] Shah, A. A., & Ribakov, Y. (2011). Recent trends in steel fibered high-strength concrete, *Materials & Design*, **32(8),** 4122-4151.

[84] Zhang, Y. Y., Harries, K. A., Yuan, W. C. (2013). Experimental and numerical investigation of the seismic performance of hollow rectangular bridge piers constructed with and without steel fiber reinforced concrete, *Engineering and Structure*, **48**, 255–265.

[85] Arslan, G. (2014). Shear strength of Steel Fiber Reinforced Concrete (SFRC) slender beams, *KSCE Journal of Civil Engineering*, **18**, No 2, 587–594.

[86] Simasathien, S., and Chao, S. H. (2015). Shear strength of steel-fiber-reinforced deep hollow- core slabs, *PCI Journal*, 85-101.

[87] ASTM. American Society for Testing and Materials. C143/143M (2003). Standard Test Method for Slump of Hydraulic Cement Concrete. ASTM International, West Conshohocken, PA.

[88] ASTM. American Society for Testing and Materials. C172/172M (1999). Standard Practice for Sampling Freshly Mixed Concrete. ASTM International, West Conshohocken, PA.

[89] ASTM. American Society for Testing and Materials. C31/C31M (2003). Standard Practice for Making and Curing Concrete Test Specimens in the Field, ASTM International, West Conshohocken, PA.

[90] ASTM. American Society for Testing and Materials. C617 (2003). Standard Practice for Capping Cylindrical Concrete Specimens, ASTM International, West Conshohocken, PA.

[91] Abbass, Ahmmad A. (2017). *Mechanical and Structural Behavior for Fiber and Engineered Cementitious Composites (ECC) Hollow Sections for Structural Members,* Ph.D study continue, Civil Engineering Department, Gaziantep University.